Geobiology

Geobiology (2014), **12**, 1–19 DOI: 10.1111/gbi.12069

Does aspartic acid racemization constrain the depth limit of the subsurface biosphere?

T. C. ONSTOTT,[1,2] C. MAGNABOSCO,[1,2] A. D. AUBREY,[3] A. S. BURTON,[4] J. P. DWORKIN,[5] J. E. ELSILA,[5] S. GRUNSFELD,[6] B. H. CAO,[7] J. E. HEIN,[7] D. P. GLAVIN,[5] T. L. KIEFT,[8] B. J. SILVER,[9] T. J. PHELPS,[10] E. VAN HEERDEN,[11] D. J. OPPERMAN[11] AND J. L. BADA[12]

[1]*Department of Geosciences, Princeton University, Princeton, NJ, USA*
[2]*Indiana Princeton Tennessee Astrobiology Initiative (IPTAI), NASA Astrobiology Institute, Indiana University, Bloomington, IN, USA*
[3]*Jet Propulsion Laboratory, California Institute of Technology, Pasadena, CA, USA*
[4]*Astromaterials Research and Exploration Science Directorate, NASA Johnson Space Center, Houston, TX, USA*
[5]*Division of Solar System Exploration, NASA Goddard Space Flight Center, Greenbelt, MD, USA*
[6]*River Hill High School, Clarksville, MD, USA*
[7]*Department of Chemistry and Chemical Biology, School of Natural Sciences, University of California-Merced, Merced, CA, USA*
[8]*Department of Biology, New Mexico Institute of Mining and Technology, Socorro, NM, USA*
[9]*ARCADIS US, Inc., Cranbury, NJ, USA*
[10]*Division of Biosciences, Oak Ridge National Laboratory, Oak Ridge, TN, USA*
[11]*Department of Microbial, Biochemical and Food Biotechnology, University of the Free State, Bloemfontein, South Africa*
[12]*Division of Geosciences Research, Scripps Institution of Oceanography, University of California, San Diego, CA, USA*

ABSTRACT

Previous studies of the subsurface biosphere have deduced average cellular doubling times of hundreds to thousands of years based upon geochemical models. We have directly constrained the *in situ* average cellular protein turnover or doubling times for metabolically active micro-organisms based on cellular amino acid abundances, D/L values of cellular aspartic acid, and the *in vivo* aspartic acid racemization rate. Application of this method to planktonic microbial communities collected from deep fractures in South Africa yielded maximum cellular amino acid turnover times of ~89 years for 1 km depth and 27 °C and 1–2 years for 3 km depth and 54 °C. The latter turnover times are much shorter than previously estimated cellular turnover times based upon geochemical arguments. The aspartic acid racemization rate at higher temperatures yields cellular protein doubling times that are consistent with the survival times of hyperthermophilic strains and predicts that at temperatures of 85 °C, cells must replace proteins every couple of days to maintain enzymatic activity. Such a high maintenance requirement may be the principal limit on the abundance of *living* micro-organisms in the deep, hot subsurface biosphere, as well as a potential limit on their activity. The measurement of the D/L of aspartic acid in biological samples is a potentially powerful tool for deep, fractured continental and oceanic crustal settings where geochemical models of carbon turnover times are poorly constrained. Experimental observations on the racemization rates of aspartic acid in living thermophiles and hyperthermophiles could test this hypothesis. The development of corrections for cell wall peptides and spores will be required, however, to improve the accuracy of these estimates for environmental samples.

Received 13 June 2013; accepted 6 November 2013

Corresponding author: T. C. Onstott. Tel.: 609 258 7678; fax: 609 258 1274; e-mail: tullis@princeton.edu

INTRODUCTION

Estimates of the anabolic rates of subsurface micro-organisms, often expressed as cellular doubling times, have been inferred from the time required to accrue sufficient organic carbon during metabolism to replace the *living* biomass concentration (Whitman *et al.*, 1998). The metabolic rates are derived from geochemical models of the subsurface flux of growth substrates (Whitman *et al.*, 1998; Larter *et al.*, 2003) or from geochemical models of the electron donors/acceptors sustaining microbial metabolic rates (Phelps *et al.*, 1994; D'Hondt *et al.*, 2002; Lin *et al.*, 2005). In the latter case, the doubling time is given by

$$t_{\text{cell}} = C_{\text{cell}}\, m_{\text{cell}}/(V\, \Upsilon_{\text{growth}}) \qquad (1)$$

where t_{cell} is in years, V is the sustaining metabolic rate estimated from geochemical constraints in moles of reactant L^{-1} $year^{-1}$, Υ_{growth} is the growth yield in grams dry weight of biomass (mole of reactant)$^{-1}$, C_{cell} is the concentration of microbial cells L^{-1}, and m_{cell} is the average cell mass in grams dry weight cell^{-1}.

The first reported estimate of cellular doubling times of subsurface micro-organisms was based upon studies of microbial communities in the 200-m-deep, Middendorf aquifer (Phelps *et al.*, 1994) and yielded doubling times of ~1400–150 000 years using *viable* cell abundances (1.5×10^9 cfu L^{-1}), CO_2 production rates (~1–107 nM $year^{-1}$), 1% growth yield: 1 g cellular C (mole of C metabolized)$^{-1}$, and 100 fg C cell^{-1} (open circles in Fig. 1A). Schippers *et al.* (2005), however, estimated cellular doubling times of only 0.82 (0.1–1.7) years (open bold diamond in Fig. 1A) for ~1- to 34-m-deep subseafloor sediments (Site 1227), based upon catalyzed reporter deposition fluorescence *in situ* hybridization (CARD-FISH) cell counts of $2–8 \times 10^8$ cells L^{-1} ($7–27 \times 10^{12}$ cells m^{-2}), a carbon oxidation rate from sulfate reduction of $5.2–16.1 \times 10^{-2}$ moles m^{-2} $year^{-1}$ (the principal electron-accepting metabolism), and assuming a higher yield of 6.6 g of cellular C (moles of C metabolized)$^{-1}$ (Heijnen & van Dieken, 1992) and a smaller cell mass of 19 fg C cell^{-1}. Schippers *et al.* (2005) assumed that the CARD-FISH cell counts are an accurate estimate of the active microbial community like the viable cell abundances used by Phelps *et al.* (1994).

Cellular doubling times of ~200 to ~2000 years (open diamonds in Fig. 1A) were recently reported for subseafloor sediments (Lomstein *et al.*, 2012) using samples from the same core, 1227, as studied by Schippers *et al.* (2005). Lomstein *et al.* (2012) employed a novel approach of measuring the aspartic acid concentrations and the D/L of aspartic acid in the sediment, estimating the aspartic acid racemization rate from Bada (1982) and assuming that the rate of racemization must equal to the rate of aspartic acid production in order for the aspartic acid D/L value to remain constant (an assumption of steady state). The latter assumption was justified given that the age of the sediment greatly exceeded the half-life of racemization. If there were no living bacteria in the sediment producing L-aspartic acid, then the D/L values should have risen quickly to 1.0 with increasing depth and age. This was not the case. Instead,

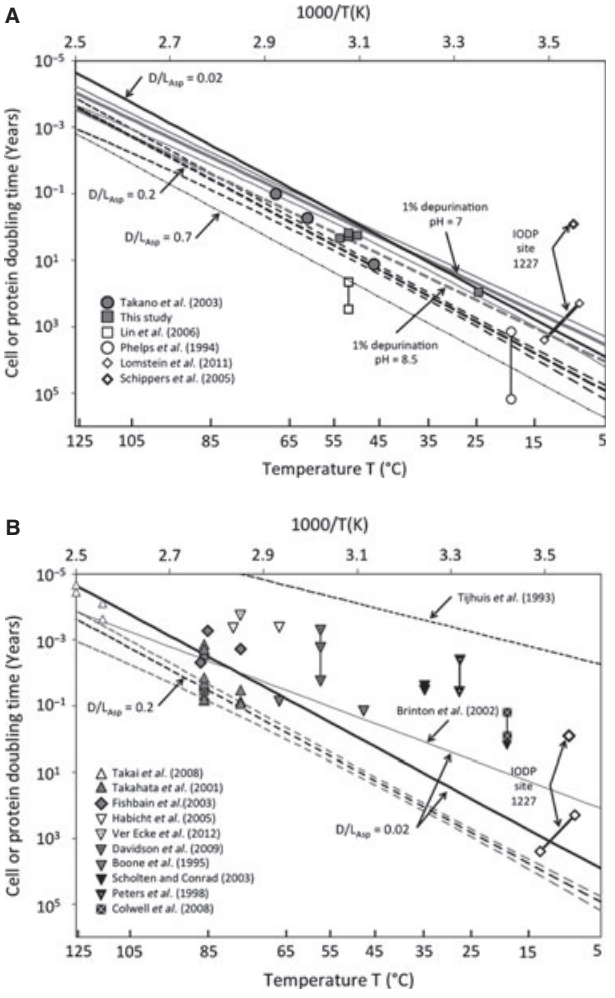

Fig. 1 (A) Arrhenius plot of protein turnover times, t_{Asp}, for a D/L of aspartic acid = 0.02 (solid black line), = 0.2 (dashed black line) and 1 SD envelope (dashed black lines) and = 0.7 (thin gray line), and of the t_{Depur} for 1% depurination at pH = 7.4 (gray solid line) and 1 SD envelope (gray solid lines) and at pH = 8.5 (dashed gray line). The $t_{\text{max}_{\text{Asp}}}$ values for South African fracture water samples (gray squares) and for water samples from Toyoha mine (gray circles) and cell doubling time for published studies (open symbols). (B) The protein turnover time extrapolated from the free aspartic acid racemization rate parameters of Brinton *et al.* (2002) and calculated assuming a D/L of aspartic acid = 0.02 (dotted line) is shown for comparison. The fit to chemostat data reported by Tijhuis *et al.* (1993) is shown (dashed black line) converted to cell doubling time using the anabolic energy requirements of McCollom & Amend (2005), and cell doubling times derived from published studies (open and closed symbols).

D/L values of aspartic acid ranged from 0.2 to 0.3 in the top 30 m of core 1227, compared to 0.08 for indigenous isolates growing at exponential phase. The concentrations of aspartic acid were $0.2–2 \times 10^{-6}$ moles (gram of sediment)$^{-1}$, and the aspartic acid racemization rate was 1.2×10^{-6} year^{-1} (B.A. Lomstein, pers. comm.). Using these figures, they calculated an aspartic acid production rate of $1–24 \times 10^{-12}$ moles of aspartic acid (gram of sediment)$^{-1}$ year^{-1}. The aspartic acid concentrations divided by these rates yield an aspartic acid turnover rate of ~10^6 years. In order to calculate a cell doubling time, however, Lomstein *et al.* (2012) had to estimate the concentration of *living* bacteria. Assuming the amino acid compositions of microbial cells and spores, the mass of active cells (170 fg C cell^{-1}) and spores (370 fg C spore^{-1}) and assuming that the *living* cell abundance is the sum of the AODC counts (10^{10}–10^{11} cells L^{-1}) and spore abundance (dipicolinic acid concentrations corresponding to 2×10^9–10^{10} spores L^{-1}), they estimated that 1.5–3% of the aspartic acid concentration was comprised of that from *living* cells or $0.3–6 \times 10^{-8}$ moles of aspartic acid (gram of sediment)$^{-1}$. Dividing this fraction by the total aspartic acid production rate yields 2500–2800 years for cellular doubling times. The same calculation but assuming a *living* cell concentration given by CARD-FISH and a cell mass of 19 fg C cell^{-1} (Schippers *et al.*, 2005), however, yields a turnover time of one year. The three orders of magnitude difference between the estimated cell turnover times reported by Lomstein *et al.* (2012) vs. Schippers *et al.* (2005) for the same samples reflects the different observations used to estimate the *living* biomass and assumptions made concerning the average cellular mass terms in equation (1).

For a single-species ecosystem at 3 km depth in continental crust, Lin *et al.* (2006) estimated that cellular doubling times were 45–300 years (open squares in Fig. 1A) based upon a geochemically deduced sulfate reduction rate of 0.2–1.5 nM year^{-1}, total cell counts of 4×10^7 cells L^{-1}, an assumed cell mass of 19 fg of C cell^{-1}, and a yield of 12.6 g of cellular C (moles of sulfate)$^{-1}$. The order of magnitude uncertainty reflects the difficulties in constraining the age of deep fracture water and thus the sulfate reduction rate. Additionally, using the total fluorescent DNA stain counts may overestimate the *living* microbial concentration.

As illustrated in the previous examples, the estimates of the cellular doubling times of subsurface micro-organisms range from less than 1 year to well over a thousand years for the temperatures encountered in the deep subsurface biosphere due to uncertainties in constraining metabolic rates and the concentration of *living* biomass. If cellular doubling times for deep subsurface prokaryotes are years to thousands of years, then depending upon the temperature, individual cells should persist long enough for the aspartic acid in their proteins to undergo significant racemization (Bada, 1982). Given that the variation in the aspartic acid racemization rate as a function of temperature is well known, the determination of the D/L-aspartic acid ratio of the amino acids from intact cells therefore should provide a direct measure of the *in situ* anabolic rate without relying upon any assumptions about the fraction of *living* biomass or the growth yield or the dominant metabolism and its rate that are required when using equation (1). Furthermore, in those environments where one type of metabolic function does dominate, the anabolic rate can provide a minimum estimate of the *in situ* metabolic rate (Stouthamer, 1979).

The goals of this study therefore were to determine (i) whether the D/L values of aspartic acid from intact cells from a deep subsurface environment exhibit a significant racemization suggestive of inactivity and a prolonged lifespan and (ii) in those cases where the dominant metabolism is established whether the measured anabolic rate when combined with amino acid concentration yields a metabolic rate consistent with geochemical models. Finally, we assessed whether the cellular protein turnover times derived from the aspartic acid racemization rate are consistent with experimentally determined survival rates for thermophiles and hyperthermophiles and, if true, could be used to constrain or explain the *living* cellular abundances near the upper temperature limit and lower depth limit of the subsurface biosphere.

METHODS

The goals of this study were accomplished by measuring the D/L values of the cellular amino acids of subsurface planktonic micro-organisms collected from the Au mines of the Witwatersrand Basin of South Africa, which currently provide access to fracture water from the deeper regions of the Earth's terrestrial biosphere. This fracture water is a mixture of paleometeoric water and Precambrian hydrothermal fluid (Lippmann *et al.*, 2003; Onstott *et al.*, 2006; Lippmann-Pipke *et al.*, 2011b) that is inhabited by microbial communities dominated by methanogens and sulfate-reducing bacteria metabolizing radiolytically generated H_2 along with sulfate derived from the oxidation of pyrite by radiolytically generated O_2 and H_2O_2 (Ward *et al.*, 2004; Gihring *et al.*, 2006; Lin *et al.*, 2006).

Fracture water sampling

We obtained five filter samples of deep subsurface water between 2001 and 2003 from three deep-level Au mines in the Carletonville area, the Driefontein, Kloof, and Mponeng Au mines, all located on the northwestern rim of the Witwatersrand Basin, South Africa (Fig. 1 in Appendix S1). With the exception of Dr938 H3 071 602, the

water came from short boreholes drilled to manage water within the mines.

Driefontein Au Mine (Gold Fields Ltd., Johannesburg, South Africa) – Driefontein Au mine is situated ~70 km west of Johannesburg. Three primary Au-bearing reefs are exploited: the Ventersdorp Contact Reef (VCR) located at the top of the Central Rand Group, the Carbon Leader Reef (CL) near the base, and the Middelvlei Reef (MR), which stratigraphically occurs some 50–75 m above the CL. The lowest working level, level 50, is 3400 m below surface. The sample Dr4 IPC 060 902 was collected from a short borehole penetrating the Transvaal Supergroup dolomite located in the intermediate pumping chamber (IPC) at 0.9 km depth of #4 shaft at Driefontein Au Mine (formerly known as East Driefontein Au mine). The IPC pumps to the surface the water that has been pumped from the 3-km-deep mining levels and is also the location where water from the regional Transvaal dolomite aquifer is used to replenish the mining water lost during recirculation. The borehole that was sampled intersects the dolomite aquifer and was sealed with a valve. The second sample from Driefontein Au Mine is Dr938 H3 071 602, which was collected from a downward-pointing exploration borehole located at 2.7 km depth with a bottom hole depth of 3.35 km and has been previously described by Moser *et al.* (2005). The borehole begins within the Ventersdorp Supergroup metavolcanic units and penetrates into the stratigraphically underlying Witwatersrand Supergroup quartzite to the MR.

Kloof Au Mine (Gold Fields Ltd.) – Two samples were collected from Kloof Au mine, which is situated ~55 km west of Johannesburg. It is comprised of seven shafts that produce Au primarily from the VCR and has been described by Kieft *et al.* (2005). Sample KL739 081 903 was collected from a 10-m-long borehole located on the 39th level of #7 shaft at a depth of 3.1 km and within the Ventersdorp Supergroup metavolcanic rock units. Sample KL441 HWDS was collected from a 4-m-long borehole located on the 41st level of #4 shaft at a depth of 3.3 km and also within the Ventersdorp Supergroup metavolcanic rock units. This borehole intersected the Glenharvie dyke, which is a major water-bearing structure for this mine.

Mponeng Au Mine (Anglo Gold Ashanti Ltd.) – One sample was collected from Mponeng Au mine, which is located ~67 km west of Johannesburg, ~8 km west of Driefontein #4 shaft. The sample MP104 H1 091 902 was collected from a short cover borehole drilled from a depth of 2.8 km along with the samples that have been described by Lin *et al.* (2006) and was extracted from the same filter utilized by Chivian *et al.* (2008) to obtain the high molecular weight DNA (>3 kb) from which the *Candidatus Desulforudis audaxviator* metagenome was sequenced.

Table 1 Site description for filter samples

Samples	Depth (kmbls)	T (°C)	pH	Salinity (ppt)	Age (Ma)	Volume through filters (L)
DR4 IPC 060902	0.945	27	7.2	0.015	0.011*	29 938
MP104 H1 091902	2.825	52	9.3	3.51	16–25†	5644
KL739 081903	3.100	54	9.5	2.67	18–23‡	7000
KL441 H2 HWDS	3.300	56	9.1	1.74	3–5‡	4927
DR938 H3 071602	3.350	54	9.1	1.00	4–53§	2504

pH and temperature were measured at the time of sampling with a portable meter.*Based upon ^{14}C analyses of DIC (Borgonie *et al.*, 2011).†Noble gas-derived ages reported from Lin *et al.* (2006).‡Noble gas-derived ages reported from Lippmann *et al.* (2003).§Noble gas-derived ages reported from Moser *et al.* (2005).

The fracture water temperature, salinity, and pH of these samples ranged from 27 to 56 °C, from 0.015 to 3.5 ppt, and from 7.5 to 9.2, respectively (Table 1). The deeper boreholes (2.8–3.4 kmbls) yielded water with the highest salinity, $\delta^{34}S$ values consistent with microbial sulfate reduction (Onstott *et al.*, 2006), $\delta^2H/\delta^{18}O$ values that were furthest removed from the meteoric water line (Ward *et al.*, 2004), and He-Xe ages of 1–25 Myr (Lippmann *et al.*, 2003), whereas the shallowest borehole, Dr4 IPC 060 902, water had the lowest salinity (0.015 ppt), δ^2H and $\delta^{18}O$ values that fell on the meteoric water line (Ward *et al.*, 2004), a ^{14}C DIC age of 10–12 kyr (Borgonie *et al.*, 2011), and δ^2H and $\delta^{13}C$ values of CH_4 and 16S rRNA gene sequence data that indicated the presence of active methanogens (Takai *et al.*, 2001; Ward *et al.*, 2004).

We used the same filtering methods as those described in Chivian *et al.* (2008). A sterile, expanding packer/manifold assembly was placed into each borehole or valved opening of the borehole and sealed to the inner casing surface. Water was allowed to flow through the manifold long enough to displace any air remaining in the borehole and manifold before connecting the filter. Samples for geochemical analyses were collected first, and then a sterile Cole Parmer double open-end pleated PTFE filter cartridge (EW-06479-52; 0.2 μm effective pore size; 8 cm diameter × 25 cm long), housed in a sterile stainless steel canister, was connected to the manifold with sterile tubing and quick connects. The filters remained attached to the borehole for several hours to more than a day. The volume of water that had passed through the filter was determined using a low flow rate totalizer (FTB300, Omega Engineering Inc., Stamford, Connecticut) attached to the outlet of the filter. Upon retrieval, the filters were quickly transferred from the stainless steel canister to a large, sterile zip-lock bag, double-bagged and placed on dry ice for transport to the field laboratory. The filters were then transported to Princeton University on dry ice and dissected under a sterile UV laminar flow hood, and ¼ of

each of the five filters was shipped frozen to Scripps Institution of Oceanography in sterile Whirlpak bags for amino acid analyses.

Amino acid analyses

Filter amino acid analyses

Amino acids were extracted from the filters, hydrolyzed, desalted, and quantified according to traditional HPLC laboratory amino acid protocols. The five filter samples were received at Scripps Institution of Oceanography and stored in a –20 °C freezer prior to analysis. Strips of the filter samples, approximately 2 cm wide and 15 cm long (~1.5 g each), were separated for analysis. The raw filter pieces were first cut into small strips with sterile surgical blades. Extractions were performed in 4 mL of double-distilled water (ddH_2O) for 24 h at 100 °C after which the supernatants were transferred into 12 × 75 mm test tubes and evaporated to dryness using a vacuum centrifuge. The dried water-extracted filter residues were vapor-phase-hydrolyzed under N_2 gas with 1 mL of 6 M HCl at 100 °C for 24 h within a 16 × 150 mm test tube. Following extraction, the hydrolyzed residues were resuspended and loaded onto equilibrated columns each packed with ~3 mL BioRad AG50W-X8 resin. Desalting was achieved following a standard amino acid desalting protocol scaled for small sample volumes (Zhao & Bada, 1995). The desalted extracts were brought to dryness and resuspended into 100 μL of ddH_2O, from which 50 μL was dried in a vacuum centrifuge with 10 μL of 0.4 M sodium borate buffer. The residues were resuspended in 20 μL of ddH_2O and derivatized with 5 μL of the fluorescent chiral adduct *o*-phthaldialdehyde/N-acetyl-L-cysteine (0.015 M OPA/NAC). After one minute, the reaction was quenched with 475 μL of 50 mM sodium acetate buffer (pH adjusted to 5.5). A 50 μL portion of the 500-μL total derivatized fraction was immediately injected after derivatization into a Rheodyne sample injection loop of a HPLC and run on a Phenomenex Luna C-18(II) 250 N-acetyl 4.6 mm column with a gradient of 50 mM sodium acetate buffer (pH = 8.5) and methanol. Samples were quantified against known standards for the amino acids, DL-aspartic acid, DL-serine, DL-glutamic acid, glycine, DL-alanine, and DL-valine. Amino acids analyzed by HPLC were identified based on retention times, and quantification was determined by normalizing the sample peak areas to those produced by standards of known concentration.

In order to quantify the amount of filtered water that each analyzed fraction represented, a new filter was weighed to determine the filter area per unit mass. The new filter (95.3 g) had an equivalent filter surface area of 0.4 m^2, and each gram was found to represent 0.0042 m^2. This number was used to normalize the mass of each analyzed filter portion (vacuum-dried mass, after extraction) to an equivalent filtered water volume using the total liters filtered (Table 1).

Amino acid analyses of standards and Escherichia coli

The D/L values of the amino acids have to be corrected for the racemization caused by hydrolysis of the cellular proteins. To do this, we processed aspartic acid, glutamic acid, serine, and alanine standards using vapor acid hydrolysis under three conditions: (i) N_2 in the head space after evacuation of the solutions, (ii) sparging of the solutions with N_2, and (iii) ambient air in the head space. The method yielding the least racemization was then used for the filters. We also processed a culture of *Escherichia coli* collected during exponential growth phase to provide an estimate of the D/L values of a *living* gram-negative bacterium (Aubrey, 2008).

Amino acid analyses of sulfate-reducing bacterium (SRB)

A *Desulfotomaculum* sp. strain PS13 (16S rRNA gene GenBank accession number KC439348) was isolated from a water sample collected from borehole MP104. The isolate was grown on medium C of Butlin *et al.* (1949) with 10 mM pyruvate as the electron donor and sulfate as the electron acceptor, N_2/CO_2 80:20 headspace, and incubation at 50 °C. Yeast extract (0.02 mL of a 10% W/V solution), 0.2 mL 5% (W/V) cysteine-HCl, 0.15 mL Wolfe's mineral solution, and 0.1 mL of Wolfe's vitamin solution (Atlas, 1993) were added anaerobically to the 7 mL of medium in a Balch tube. NaOH was used to adjust the pH of the medium to 7.5–8.0 prior to autoclaving and subsequent inoculation with 2 mL of borehole water. Isolation was performed by dilution to extinction of the inoculation and multiple transfers. Genomic analysis of the isolate revealed that 99.9% of the 80 460 SSU rRNA reads were 97% similar to the 16S rRNA gene sequence KC439348 (C. Cameron, National Center of Genomic Research, pers. comm.). After 10 days of incubation at 50 °C, cell concentrations reached ~10^8 cells mL^{-1}. In preparation for amino acid analyses, cells were collected in exponential growth phase and were pelleted by centrifugation at 10 000 × g for 2 min. The pellet was then rinsed three times, once with 1.5 mL of sterile phosphate-buffered saline (PBS) solution and twice with 3 mL of sterile ddH_2O. The cell pellet, the medium supernatant, and the sterile PBS wash solution were sent to the NASA Goddard Space Flight Center (GSFC) for amino acid analyses. Because initial results indicated that the medium contained significant concentrations of racemized amino acids, a second pellet was prepared by first transferring the isolated SRB from the yeast extract-bearing Butlin C medium to a Butlin C medium without yeast extract and with ^{15}N-labeled NH_4Cl as its sole N source. After 10 days of incubation, the isolated SRB was then transferred a second

and third time and incubated repeated for 10 days with ^{15}N-labeled NH_4Cl medium to remove any residual amino acids from yeast extract. The culture was then centrifuged at 10 000 × g for 2 min in 1 mL aliquots in two parallel 1.5-mL microcentrifuge tubes. Once the entire culture was exhausted, 4 mL of sterile PBS was added to the Balch tube to remove any residual cells and the PBS was then pelleted using the same procedure. The two pellets were then suspended with 1 mL PBS and pelleted again. The two pellets were then suspended with filtered, autoclaved ddH_2O and combined into one microcentrifuge tube. The pellet was then rinsed four times with 1 mL of sterile ddH_2O. The ^{15}N-labeled cell pellet, the ^{15}N-labeled medium, the sterile PBS, and sterile ddH_2O were then sent to NASA GSFC for amino acid analyses.

At GSFC glassware was heated to 500 °C in air to sterilize and remove organic contaminants. A pellet of the SRB was suspended in 1 mL of Millipore Milli-Q Integral 10 (18.2 MΩ, <3 parts per billion total organic carbon) ultrapure water and resuspended by vortexing for 1 min. An aliquot of 250 μL of the cell suspension was extracted in parallel with PBS solution, ^{15}N growth medium, and procedural blanks of water from NASA GSFC and Princeton University. Extractions were performed in sealed ampoules heated at 100 °C for 24 h. The extracted supernatants were collected, dried under vacuum, and then acid-vapor-hydrolyzed (6M HCl) at 100 °C for 24 h to liberate bound amino acids. Following hydrolysis, the samples were desalted by cation-exchange chromatography using columns prepacked with BioRad AG50W-X8 100- to 200-mesh resin. Amino acids were eluted with 2M NH_4OH produced *in vacuo* from gaseous NH_3 and ultrapure water. After desalting, samples were derivatized with OPA/NAC containing either *N*-acetyl-L-cysteine or *N*-acetyl-D-cysteine. The OPA/NAC derivatives were separated using a Waters BEH C18 column (2.1 × 50 mm, 1.7 μm particle size) followed by a Waters BEH phenyl column (2.1 × 150 mm, 1.7 μm particle size) with gradients tuned for general separation (Glavin *et al.*, 2010). The electrospray and mass spectrometer (Waters ACQUITY UltraPerformance and Waters Premier LC-FD/TOF-MS, or Waters Quattro micro API LC-QqQ-MS, Waters Corporation, Milford, MA, USA) conditions have been described (Glavin *et al.*, 2006). Amino acids in the samples were identified by correlating sample compounds with known amino acid standards using the masses of the OPA/NAC amino acid derivatives and chromatographic retention times using both mass and fluorescence detection.

Synthesis of N-Acetyl-D-Cysteine

A solution of MeOH and 0.1M $NaPO_4$ buffer (231 mL MeOH: 154 mL Na_3PO_4 solution) was degassed by bubbling N_2 through the sample for 25 min. D-Cysteine (10 g, 83.0 mmol) was then dissolved in the degassed $MeOH/Na_3PO_4$ solution. The reaction was acidified with concentrated H_3PO_4 (pH ≈ 6). CH_3CN (40 mL, 766 mmol) was added, and the sample was heated to reflux under a N_2 atmosphere for 3 days. The sample was concentrated to ~1/5 the original volume under vacuum, and the resulting solution was acidified with concentrated H_3PO_4 (pH ≈ 2). The sample was stirred until a precipitate formed. The slurry was filtered and then the precipitate was washed with water (~2 × 15 mL). The crude solid was dissolved in MeOH and filtered to remove any insoluble material. The MeOH was removed under vacuum to yield D-*N*-acetylcysteine (12 g, 73.5 mmol, 89%) as a white crystalline material. Crystals were dissolved in ddH_2O to a final concentration of 10^{-6} M, and the mass of *N*-acetyl-D-cysteine was confirmed by MALDI-TOF (calculated mass for $C_5H_9NO_3S$ $[M+H^+]$ of 164.03; measured to be 164.01). The structure was confirmed by 1H NMR (*d4*-MeOD, 400 MHz) δ 2.02 (3H, s), 2.81 (1H, dd, J_1 = 13.9 Hz, J_2 = 6.4 Hz, -C*H*H-), 2.95 (1H, dd, J_1 = 13.9 Hz, J_2 = 4.4 Hz, -CH*H*-), 4.59 (1H, dd, J_1 = 6.3, J_2 = 4.5 Hz) (Glavin *et al.*, 2006).

Model parameters and calculations

The equivalent cellular concentrations were calculated from total amino acids, ΣAA, assuming that the quantified amino acids represent 70% of the total bacterial protein (Glavin *et al.*, 2001), a microbial cell protein content of 55% by mass (Stouthamer, 1979), and a mass of each cell of 19 fg (Schippers *et al.*, 2005) according to the following equation:

$$\begin{aligned}\text{Cells mL}^{-1} &= \text{AA g mL}^{-1}/\text{AA g cell}^{-1} \\ &= \Sigma\text{AA}/(0.7 \cdot 0.55 \cdot 19{\times}10^{-15})\end{aligned} \quad (2)$$

Equation (2) is only used to provide a comparison between the amino acid concentrations and other estimates of the prokaryotic cellular abundance of the fracture water samples and is not utilized in the racemization model described below.

Amino acid racemization occurs when a hydroxide ion removes a proton from the α-carbon resulting in the formation of a carbanion intermediate (Bada, 1982). The carbanion intermediate subsequently reacts with H_2O to acquire a proton. The first step is the rate-limiting step and follows a simple first-order reaction law with respect to amino acid concentration. For peptide- and protein-bound amino acids, the racemization rate is independent of pH in the region of pH = 6–9 (Bada, 1982). A simple numerical mass balance model for the reaction was implemented utilizing the following equations:

$$[\mathrm{L-AA}]_{t+\mathrm{d}t} = [\mathrm{L-AA}]_t + \{k_{\mathrm{TO}} \cdot [\mathrm{L-AA}]_t + k_{\mathrm{RAC}} \cdot [\mathrm{D-AA}]_t - k_{\mathrm{RAC}} \cdot [\mathrm{L-AA}]_t\} \cdot \mathrm{d}t \quad (3)$$

$$[\mathrm{D-AA}]_{t+\mathrm{d}t} = [\mathrm{D-AA}]_t + \{k_{\mathrm{RAC}} \cdot [\mathrm{L-AA}]_t - k_{\mathrm{RAC}} \cdot [\mathrm{D-AA}]_t\} \cdot \mathrm{d}t \quad (4)$$

where k_{TO} is the first-order rate of cellular amino acid turnover (year^{-1}) and k_{RAC} is the amino acid racemization rate (year^{-1}). This model assumes that any D-amino acids, [D-AA], are formed from racemization of the L-amino acids, [L-AA], and vice versa. Because the racemization rate of aspartic acid is best known and the highest, this model was applied only to the aspartic acid analyses. The degradation rate of the D- and L-amino acids is assumed to be negligible because the rates associated with racemization are generally >100× faster than amino acid degradation (Li & Brill, 2003).

Because the goal of this model is to determine the cellular protein turnover time for *living* bacteria, the *in vivo* racemization rate for aspartic acid was used as opposed to the racemization rate for free aspartic acid (Bada, 1982). The *in vivo* racemization rate constants were extrapolated to the borehole water temperatures using an Arrhenius relationship and the *in vivo* racemization rate data from Masters *et al.* (1977), which are similar to the rates reported by Bada *et al.* (1999) and Rosa *et al.* (2012). The extrapolated *in vivo* racemization rate, k_{Asp}, was calculated using Arrhenius parameters and the following equation:

$$k_{\mathrm{Asp}} = k_{T_1} e^{\frac{E_A(T_2 - T_1)}{RT_1T_2}} \quad (5)$$

where $k_{T_1} = 1.3 \pm 0.3 \times 10^{-3}$ year^{-1}, $T_1 = 310.15$ K (37 °C), $E_A = 35 \pm 2$ kcal mole^{-1}, $R = 0.001\,986$ kcal mole^{-1} K^{-1}, and T_2 is the *in situ* temperature in K.

A steady state of amino acid production and racemization is assumed to exist in these fracture water sites, given that the estimated ages of the bulk water (Table 1) exceed the ten- to thousand-year half-lives (Bada, 1982) for aspartic acid racemization at these temperatures. In the case of the numerical model, the k_{TO} was manually adjusted until the D/L ratio of aspartic acid stabilized and matched that of the measured D/L ratio of the measured aspartic acid. The steady-state assumption that the D/L ratio is constant, $\mathrm{d(D/L)_{Asp}}/\mathrm{d}t = 0$, requires that the rate of newly produced L-aspartic acid matches the rate of D-aspartic acid production by racemization. The following expression for the cellular protein turnover rate, k_{TO}, is derived by differentiating the ratio of equations (3) and (4) (see Appendix S1),

$$k_{\mathrm{TO}} = k_{\mathrm{Asp}} \cdot (1 + (\mathrm{D/L})_{\mathrm{Asp}}) \cdot ((\mathrm{L/D})_{\mathrm{Asp}} - 1) \quad (6)$$

The cellular protein concentration increases exponentially at the rate k_{TO} for which the turnover or doubling time, t_{Asp}, is given by

$$t_{\mathrm{Asp}} = \ln 2 / k_{\mathrm{TO}} \quad (7)$$

Because exponential growth is not expected in deep subsurface environments, the protein generation rate was also treated as a zero-order constant and matched by a zero-order protein decay associated with cell death and release of the protein into the extracellular pool. The expression for k_{TO} in this case is also derived in the Appendix S1 and is as follows:

$$k_{\mathrm{TO}} = k_{\mathrm{Asp}} \cdot ((\mathrm{L/D})_{\mathrm{Asp}} - 1) \quad (8)$$

For $D_{\mathrm{Asp}}/L_{\mathrm{Asp}} \ll 1$, the k_{TO} of equation (6) is virtually identical to the k_{TO} of equation (8) as confirmed by numerical modeling. Equations 6–8 assume that the D/L values of aspartic acid have already been corrected for racemization during acid hydrolysis of the cellular proteins and peptides during sample preparation. We corrected the measured D/L values for acid hydrolysis using the following equations from Kaiser & Benner (2005),

$$[\mathrm{L\text{-}Asp}]_0 = \{[\mathrm{L\text{-}Asp}] - [\mathrm{D\text{-}Asp}](\mathrm{D/L})_{\mathrm{exp}}]\}/[1 - (\mathrm{D/L})_{\mathrm{exp}}] \quad (9)$$

and

$$[\mathrm{D\text{-}Asp}]_0 = [\mathrm{D\text{-}Asp}] + [\mathrm{L\text{-}Asp}] - [\mathrm{L\text{-}Asp}]_0 \quad (10)$$

where $(\mathrm{D/L})_{\mathrm{exp}}$ is the D/L ratio of an L-aspartic acid standard after acid hydrolysis, [L-Asp] and [D-Asp] are the measured concentrations of D- and L-aspartic acid of the sample, and $[\mathrm{L\text{-}Asp}]_0$ and $[\mathrm{D\text{-}Asp}]_0$ are the concentrations of the D- and L-aspartic acid after correction for acid hydrolysis. Using these corrected values, we define a minimum aspartic acid turnover rate, $k_{TO'}$, and maximum turnover time, $t_{\mathrm{max}_{\mathrm{Asp}}}$, as follows,

$$k_{\mathrm{TO'}} = k_{\mathrm{Asp}} \cdot ((\mathrm{L_0/D_0})_{\mathrm{Asp}} - 1) \quad (11)$$

$$t_{\mathrm{max}_{\mathrm{Asp}}} = \ln 2 / k_{\mathrm{TO'}} \quad (12)$$

A further correction to the D/L ratio of aspartic acid must be made for any D-aspartic acid residues present in

the cell walls. This is particularly important for gram-positive bacteria where 26–75 wt% of the total cell dry weight is comprised of cell wall polymers and 7–56 wt% of the cellular amino acids is comprised of peptides from the cell wall peptidoglycan and teichoic acid and from S-layer glycoproteins (van der Wal *et al.*, 1997). Peptidoglycan usually contains short cross-linking peptide containing L-alanine, D-glutamic acid, L-lysine, and D-alanine. Usually when two peptide sequences link, one of the D-alanine molecules is released. Gram-positive bacteria also possess secondary cell wall polymers known as teichoic acids, which also contain D-alanine (Willey *et al.*, 2011). The composition of these cross-linking peptide bonds of peptidoglycan, however, is highly variable (Schleifer & Kandler, 1972), and D-aspartic acid has been reported in the peptidoglycan of *Streptococcus faecium* and *Lactobacillus casei* (Staudenbauer, 1968) with a D/L-aspartic acid of 3.3 (Grutters *et al.*, 2002). The gram-negative bacteria contain a lower proportion of peptidoglycan than the gram-positive bacteria, and the cell walls of certain Archaeal species, for example methanogens, are composed of pseudo-peptidoglycan, which does not contain D-amino acids (Kandler & Konig, 1978). Matsumoto *et al.* (1999) have claimed, however, that D-aspartic acid is produced in Archaeal *Thermococcus* strains although its function remains uncertain. Given the variability of cell wall composition as a function of taxonomy and, to a lesser extent, environmental conditions, an accurate correction of the D/L ratio of a cell's aspartic acid for the aspartic acid D/L of its cell wall is challenging. One approach, used by Lomstein *et al.* (2012) and adopted here, is to determine the aspartic acid D/L of isolates derived from the same samples and equations (9) and (10). With this correction, the resulting t_{Asp} value would be less than $t_{max_{Asp}}$.

The protein turnover time must be supported by a sufficiently high microbial metabolic rate. The total cellular amino acid concentration is a measure of the total protein concentration and the cell wall amino acid content. Depending upon the carbon substrate utilized by the microbial community, synthesizing one gram of protein requires the consumption of at least 21×10^{-3} moles of ATP for glucose, 43×10^{-3} moles of ATP for acetate, and 91×10^{-3} moles of ATP for CO_2 ignoring the energetic costs of cross-membrane transport and mRNA turnover (Stouthamer, 1979). The protein yield per mole of ATP is referred to here as $1/Y_{ATP}$. A specific metabolic reaction will yield a certain proportion of ATP, m_{ATP} in moles of ATP (moles of reactant)$^{-1}$, for example, sulfate reduction coupled to H_2 oxidation reaction yields 1.3 moles of ATP per mole of sulfate reduced (Jin & Bethke, 2005). The *in situ* metabolic rate, V (moles of reactant L^{-1} year^{-1}), therefore is given by the following expression:

$$V = k_{TO}\,\Sigma AA/(0.7\,Y_{ATP}\,m_{ATP}) \quad (13)$$

where $\Sigma AA = \Sigma Asp + Glu + Ser + Gly + Ala + Val$ and $\Sigma AA/0.7$ is the estimated total amount of cellular protein. The rate of ATP consumption is a biospeedometer for metabolic activity. If the principal metabolic pathway is known and the carbon substrate is known, then one can calculate the minimum rate of ATP production from the cellular protein turnover rate. The minimum rate required for cell turnover is approximately double this rate (Stouthamer, 1979).

For comparison purposes, the cellular protein turnover times, t_{cell}, were calculated using (i) expression (1) above for data derived from published chemostat experiments (VerEecke *et al.*, 2012), survival experiments (Boone *et al.*, 1995; Takahata *et al.*, 2001; Takai *et al.*, 2008), and (ii) calculated from the cell-specific minimum metabolic rates of chemostat experiments (Tijhuis *et al.*, 1993; Habicht & Canfield, 1996; Peters *et al.*, 1998; Scholten & Conrad, 2000; Habicht *et al.*, 2005) and retentostat experiments (Colwell *et al.*, 2008; Davidson *et al.*, 2009) by substituting them in for V in equation (13) and solving for k_{TO}.

The t_{cell} values of Colwell *et al.* (2008) were based on one measurement of the autotrophic CH_4 production rate per cell and one yield value for autotrophy, plus two different assumptions regarding the cell mass (20 fg vs. 100 fg – solid squares with crosses in Fig. 1B). The t_{cell} values for the Habicht *et al.* (2005) experiments were calculated from their results and assuming 1.3 moles of ATP per mole of sulfate reduced and 2.05×10^{-4} of ATP per g of protein produced. The t_{cell} values for Davidson *et al.* (2009) were calculated from the retentostat experimental rates using the same parameters and assuming a 20 fg cell mass consistent with TEM images. The t_{cell} values of VerEecke *et al.* (2012), Peters *et al.* (1998), and Scholten & Conrad (2000) were cited directly from their conclusions.

RESULTS AND DISCUSSION

Amino acid analyses of standards and isolates

The degree of racemization observed for aspartic acid, glutamic acid, and alanine standards during acid vapor hydrolysis was less when performed with a head space gas of N_2 following evacuation of the solution compared to when with the solution was sparged with N_2 or with a head space gas of ambient air (Table 2). The degree of racemization of serine was $0.7 \pm 0.2\%$ and identical for all three approaches. The degree of racemization of aspartic acid was 0.4–0.7% during hydrolysis under a N_2 headspace following evacuation of the solution vs. 0.7–1.7% under ambient air conditions. These degrees of racemization are considerably less than those reported by Kaiser & Benner (2005) with the exception of serine. Kaiser & Benner

Table 2 Degree of racemization caused during hydrolysis (6 M HCl, 24 h, 100 °C) for several proteinogenic amino acids

Treatment	Aspartic acid*	Glutamic acid*	Serine†	Alanine†
N_2 (vacuum-evacuated)	0.4–0.7%	0.10.2%	0.7 ± 0.2%	0.6 ± 0.2%
N_2 (blown into tube)	0.6–2.0%	0.5–0.6%	0.7 ± 0.2%	1.2 ± 0.2%
Ambient air	0.7–1.7%	0.6–0.7%	0.7 ± 0.2%	1.4 ± 0.3%

*Values given are the range of two measurements. Due to a lack of baseline separation between enantiomers, data were only used from runs where the minor enantiomer was the first compound to elute. For aspartic acid, this was the L-NAC derivatization, and for glutamic acid, this was the D-NAC derivatization.†Values given are the average and standard error from four measurements, two with each of D- and L-NAC.

(2005) reported that the fraction of D-aspartic acid produced during microwave vapor-phase hydrolysis was 9.4 ± 0.4% and during liquid-phase hydrolysis was 4.4 ± 0.1%.

The *E. coli* culture yielded D/L values of 0.02 for aspartic acid, glutamic acid, serine, and valine and 0.05 for alanine (Table 3). Correcting the D/L ratio of aspartic acid for acid hydrolysis yields a D_0/L_0 of 0.013 to 0.016 for the *E. coli* culture. This range of values is comparable to that reported for a gram-negative marine phototrophic bacterium, *Synechococcus bacillaris*, by Kaiser & Benner (2005), who measured a D/L ratio of 0.04 for aspartic acid, which was equivalent to a D_0/L_0 value of 0.007 to −0.02 after correction for their liquid-phase hydrolysis. Lomstein *et al.* (2012) reported a much higher average D/L value of 0.086 ± 0.024 for four strains of gram-negative bacteria isolated from seafloor sediments, but they did not state whether these values had been corrected for acid hydrolysis.

The initial amino acid analyses of the thermophilic *Desulfotomaculum* strain PS13 revealed a very high D_0/L_0 value of aspartic acid of 0.23–0.24, but also revealed very high concentrations of amino acids in the medium with even higher D/L values. We sought to eliminate any carryover of racemized amino acids from the yeast extract by performing multiple transfers in a medium with $^{15}NH_4Cl$ as the sole nitrogen source (yeast extract was omitted) before pelleting and rinsing the cells. The proportion of ^{15}N in the aspartic acid was 92%, indicating that almost all of the N was derived from the labeled substrate, and the resulting D_0/L_0 value of the aspartic acid was 0.17–0.18 (Table 4; Fig. 2). The D/L ratio of the aspartic acid in the medium was 0.75, and it contained no detectable ^{15}N. Assuming that the 8% ^{14}N of aspartic acid was residual aspartic acid from the original yeast-bearing medium, then the D_0/L_0 value for the aspartic acid becomes 0.11–0.12 (Table 3).

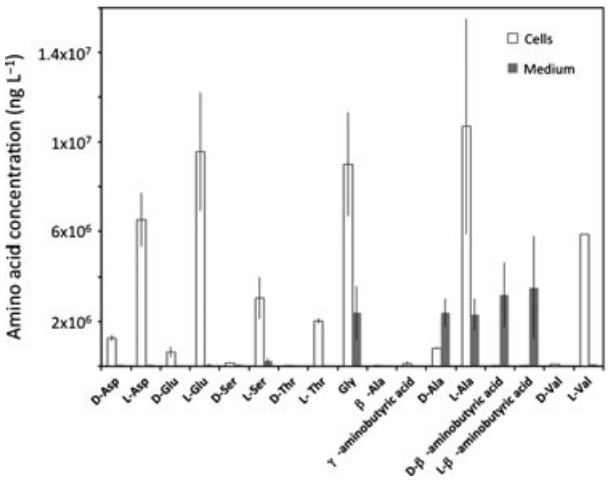

Fig. 2 Concentrations (ng L^{-1}) of amino acids in extract from ^{15}N-grown *Desulfotomaculum* strain PS13 cells and medium.

Although the ^{15}N-labeled medium yielded much lower amino acid concentrations than the cells (Fig. 2), it contained ^{15}N-enriched D-glutamic acid (73%), D-alanine (66%), L-alanine (64%), L-valine (70%), and D- and L-β-amino-*n*-butyric acid (54%), all of which are components of gram-positive peptidoglycan (Schleifer & Kandler, 1972). The D_0/L_0 value for the extracellular alanine was 1.03 vs. the 0.06–0.07 for the cellular alanine, which could be explained by teichoic acid components that separated from the cell walls during incubation and growth or pelleting.

Table 3 Amino acid D/L values of filter samples and isolates

Sample	D/L-Asp	D/L-Glu	D/L-Ser	D/L-Ala	D/L-Val
Escherichia coli	0.02	0.02	0.02	0.05	0.02
Desulfotomaculum str. PS13	0.19	0.07	0.05	0.08	0.01
Medium	0.75	0.25	0.26	1.04	0.14
Desulfotomaculum str. PS13*	0.11–0.12	0.018–0.019	−0.008 to −0.012	n.d.	n.d.
DR4IPC	0.044	0.063	0.053	0.358	<0.03
DR938	0.054	0.084	0.048	0.554	0.205
MP104	0.049	0.065	0.049	0.252	0.025
KL739	0.065	0.060	0.046	0.503	<0.03
KL441	0.098	0.084	0.086	0.437	0.027

*D/L values corrected using the proportion of ^{15}N and for acid hydrolysis.

Table 4 Amino acid concentrations (ng L^{-1}) and%^{15}N for sulfate-reducing thermophilic bacterial cells and $^{15}NH_4Cl$-labeled growth medium

Amino acid	Cells	%^{15}N	Medium	%^{15}N
D-Aspartic acid	$1.3 \pm 0.1 \times 10^6$	<d.l.	$5.5 \pm 2.5 \times 10^4$	<d.l.
L-Aspartic acid	$6.5 \pm 1.2 \times 10^6$	92	$7.3 \pm 0.9 \times 10^4$	<d.l.
D-Glutamic acid	$6.3 \pm 2.4 \times 10^5$	81	$1.8 \pm 0.3 \times 10^4$	73
L-Glutamic acid	$9.6 \pm 2.6 \times 10^6$	79	$7.1 \pm 5.3 \times 10^4$	40
D-Serine	$1.6 \pm 0.2 \times 10^5$	83	$6.3 \pm 4.1 \times 10^4$	14
L-Serine	$3.1 \pm 1.0 \times 10^6$	81	$2.4 \pm 1.2 \times 10^5$	5
D-Threonine	$<1.2 \times 10^4$	<d.l.	$<1.2 \times 10^4$	<d.l.
L-Threonine	$2.0 \pm 0.1 \times 10^6$	<d.l.	$<1.2 \times 10^4$	<d.l.
Glycine	$9.0 \pm 2.3 \times 10^6$	79	$2.4 \pm 1.2 \times 10^6$	33
β-Alanine	$4.1 \pm 0.6 \times 10^4$	70	$3.2 \pm 0.4 \times 10^4$	34
γ-Amino-*n*-butyric acid	$1.3 \pm 1.1 \times 10^5$	<d.l.	$<1.0 \times 10^4$	<d.l.
D-Alanine	$8.2 \pm 0.4 \times 10^5$	66	$2.4 \pm 0.6 \times 10^6$	66
L-Alanine	$1.1 \pm 0.5 \times 10^7$	60	$2.3 \pm 0.7 \times 10^6$	64
D-β-Amino-*n*-butyric acid	$<1.0 \times 10^4$	<d.l.	$3.2 \pm 1.4 \times 10^6$	54
L-β-Amino-*n*-butyric acid	$<1.0 \times 10^4$	<d.l.	$3.5 \pm 2.3 \times 10^6$	54
D-Valine	8.2×10^4	50	$<1.2 \times 10^4$	<d.l.
L-Valine	5.9×10^6	63	8.20×10^4	70

The D_0/L_0 value for aspartic acid of 0.11–0.12 for *Desulfotomaculum* strain PS13 is significantly greater than that reported for gram-positive *Bacillus subtilis* by Kaiser & Benner (2005), who measured a D/L value of 0.07 for aspartic acid, equivalent to a D_0/L_0 value of 0.01 to 0.04 after correction for their liquid-phase hydrolysis. Lomstein *et al.* (2012) reported an average D/L ratio of 0.084 ± 0.020 for three strains of gram-positive bacteria isolated from seafloor sediments, but they did not state whether these values had been corrected for acid hydrolysis.

Amino acid analyses of filter samples

The total hydrolyzed cellular amino acid (ΣAA = ΣAsp + Glu + Ser + Gly + Ala + Val) concentrations ranged from 5.8 to 471 ng L^{-1} (Table 5). Based upon equation (2), these concentrations correspond to 7.9×10^5–6.4×10^7 cells L^{-1}, in general agreement with flow cytometry counts of SYTO13-DNA-stained cells of 5×10^5–3.3×10^7 cells L^{-1} (Table 5) (Pfiffner *et al.*, 2006), although sample-to-sample agreement varies considerably. The total aspartic acid concentration ranged from 1.4×10^{-15} to 1.1×10^{-13} moles mL^{-1} or 7–9 orders of magnitude less than the 0.2–2×10^{-6} moles (gram of sediment)$^{-1}$ reported by Lomstein *et al.* (2012) for seafloor sediment.

The relative amino acid concentrations are all highly similar to those of *living* bacterial communities mostly consisting of L-amino acids, D/L values less than 0.1, with the exception of alanine for which the D/L values were greater than 0.3. The D/L values of aspartic acid ranged from 0.044 to 0.098 (Table 3). After correcting for the racemization due to acid hydrolysis, the D_0/L_0 values of aspartic acid ranged from 0.037 to 0.095 (Table 6). The maximum turnover times for the cellular amino acid pool, $t_{max_{Asp}}$, calculated using equation (12) ranged from 137–148 (−22/+25) years for Dr4IPC, the coolest fracture water, to 1.4–2.1 (±0.4) years for the other boreholes whose temperatures ranged from 52 to 56 °C (gray squares in Fig. 1A). The D_0/L_0 values of the filter samples are all less than that of the *Desulfotomaculum* strain PS13, which even though isolated from borehole MP104 was a species that was never detected in the 16S rRNA gene sequence libraries for any of the sampled boreholes (Gihring *et al.*, 2006). Firmicutes are the dominant phylotype of boreholes MP104, KL441, KL739, and Dr938, however, and the measured D_0/L_0 values of aspartic acid could largely reflect cell wall composition, in which case the true cellular protein turnover times would be much less than a year. Gram-negative Proteobacteria are the dominant phylotypes of borehole Dr4IPC (Gihring *et al.*, 2006). Therefore, if we use our measured D_0/L_0 values of aspartic acid for *E. coli* to correct for cell wall D-aspartic acid, the revised D_0/L_0 values become 0.023–0.026 and the cellular protein turnover time decreases to 82–94 (−14/+15) years (gray square in Fig. 1A). The error in these estimates is one standard deviation and is a combination of the error in the corrected D/L values and the error in the aspartic acid racemization rate.

Table 5 Amino acid concentrations (ng L^{-1}) and equivalent cellular concentrations and flow cytometry counts (cells L^{-1})

Sample	D-Asp	L-Asp	D-Glu	L-Glu	D-Ser	L-Ser	Gly	D-Ala	L-Ala	D-Val	L-Val	TOTAL*	10^6 cells L^{-1}†	10^6 cells L^{-1}‡
DR4IPC	0.0317	0.72	0.034	0.54	0.079	1.51	1.30	0.29	0.81	0.0096	0.45	5.77	0.79	11
DR938	0.172	3.22	0.174	2.08	0.399	8.40	4.64	2.20	4.08	0.400	1.96	27.73	3.8	3.6
MP104	0.260	5.28	0.213	3.25	0.728	14.76	9.28	2.22	8.92	0.074	2.91	47.9	6.6	33.0
KL739	0.190	2.91	0.086	1.42	0.322	7.09	6.34	1.55	3.15	0.048	6.80	29.9	4.1	4.1
KL441	5.08	51.6	3.73	44.4	9.40	110	85.2	33.1	77.2	1.36	50.0	471	64.0	0.5

*Σ = Asp, Glu, Ser, Gly, Ala, Val.†Equivalent cellular concentrations assuming that quantified amino acids represent 70% of total bacterial protein[25], a cell mass of 19 fg per cell[4], and 55% protein per cell by dry weight[26]. This number was multiplying the amount of amino acid extracted by 4 because the amino acids were extracted from ~¼ of the filter and then dividing by the water volume (Table 1).‡Flow cytometry counts using cyto13 DNA stain or PLFA concentrations (pmol L^{-1}) × 2.5×10^4.

Table 6 Cellular protein turnover times from D_0/L_0 values of aspartic acid

Sample	T_2 (K)	k_{T_2} (year^{-1})	D_0/L_0-Asp	$t_{max_{Asp}}$ −/+ 1 SD(year)	V (nM year^{-1})
Dr4IPC	300	1.9×10^{-4}	0.037–0.040*	137–148 (−22/+25)†	N.A.
MP104	325	1.7×10^{-2}	0.042–0.045	1.7–1.8 (−0.3/+0.4)	2.4 (+1.0/−0.8)
KL739	327	2.4×10^{-2}	0.058–0.061	1.7–1.8 (−0.4/+0.3)	1.5 (+0.8/−0.3)
Dr938	327	2.4×10^{-2}	0.047–0.050	1.4–1.5 (−0.3/+0.3)	1.8 (+1.0/−0.4)
KL441	329	3.3×10^{-2}	0.092–0.095	2.0–2.1 (−0.3/+0.5)	21 (+4/−5)

$$\ln\left(\frac{k_{T_2}}{k_{T_1}}\right) = \frac{E_A \cdot (T_2 - T_1)}{R \cdot T_1 \cdot T_2}$$

$k_{T_1} = 1.3 \pm 0.3 \times 10^{-3}$ year^{-1} at 37 °C

$E_A = 35 \pm 2$ kcal mole^{-1}

$R = 0.001\ 986$ kcal mole^{-1} K^{-1}

Cellular protein turnover times, t_{Asp}, were calculated assuming steady state (i.e. constant $(D/L)_{Asp}$) and $\ln(2)/t_{max_{Asp}} = \ln(2)/k_{TO} = \ln(2)/\{k_{T_2}\ [(L_0/D_0)_{Asp} - 1]\}$. The error in t_{Asp} is derived in the Supporting Information. *In situ* microbial metabolic rate, V, was calculated from sulfate reduction and assuming CO_2 as the carbon substrate and $V = k_{TO}\ \Sigma AA/(0.7\ Y_{ATP}\ m_{ATP})$.*Correcting for the cell wall proteins using the *E. Coli* analyses yields a D_0/L_0-Asp of 0.023–0.026.†The cellular protein turnover time decreases to 82–94 (−14/+15) years after correcting for cell wall proteins using the *E. coli* analyses.

The amino acid compositions and D/L values obtained in this study are quite similar to the results of a pioneering investigation of a 550-m-deep hydrothermal system located in Toyoha mine by Takano *et al.* (2003). That study's water samples yielded D/L values of 0.05–0.15 for aspartic acid, which correspond to t_{Asp} values of 13–0.1 years given the *in situ* temperatures ranging from 48 to 71 °C (gray circles in Fig. 1A). Unfortunately, these are maximum estimates given that Takano *et al.* (2003) did not report how much racemization occurred during their acid hydrolysis and that the amino acids were extracted from the bulk water sample, meaning that it included both cellular and extracellular amino acids. Nonetheless, their total amino acid concentrations, which ranged from 2×10^5 to 6×10^5 ng L^{-1}, agree with their total cell counts of ~10^{10} cells L^{-1}. Their most abundant amino acids were serine and glycine, similar to our samples. The proportion of the total amino acid pool comprising aspartic acid, glutamic acid, serine, glycine, alanine, and valine was 0.64 ± 0.12, which is within error of our assumed value of 0.7. The one significant difference between their results and ours was the D/L values of alanine, which ranged from 0 to 0.06, whereas ours ranged from 0.3 to 0.6 (Table 3), perhaps because of a microbial community composition difference that results in less cell wall alanine.

Our results indicate that the D/L values of aspartic acid in the cellular amino acids of deep subsurface planktonic micro-organisms are very low, ~0.02 in the case of sample Dr4IPC. Experiments studying the effects of racemization of aspartic acid and asparagine (which deamidates through a highly racemic intermediate) on the enzymatic activity of lysozymes, RNAse A and synthetic peptides have shown that a significant irreversible structural damage and inactivation of protein enzymes occur for D/L values as low as 0.02 (Hayashi & Kameda, 1980; Geiger & Clarke, 1987; Tomizawa *et al.*, 1995; Zhao & Bada, 1995). Irreversible thermal inactivation of proteins occurs by many other mechanisms (Vieille & Zeikus, 2001), but for proteins that are supposed to remain stable and active for long periods of time without replacement, the aspartic acid and asparagine residues are the weakest link in the peptide chain due to their racemization.

Aspartic acid comprises 6.1%, 5.8%, and 5.2% of the protein structures of mesophiles, thermophiles, and hyperthermophiles, respectively (Greaves & Warwicker, 2007). This small decline with increasing growth temperature reflects a preference for glutamic acid over aspartic acid that is related to the thermal stability of exposed ionizable amino acid groups. This implies that the proteins of hyperthermophiles are as vulnerable to aspartic acid racemization as mesophiles. Some actively growing cultures of hyperthermophilic Archaea contain 43–49% D-aspartic acid in the free aspartic acid pool (Matsumoto *et al.*, 1999), and because this free aspartic acid pool comprises only 0.3% by mass of the total protein amino acid pool, the free D-aspartic acid could be in part produced by racemization. Aspartate racemase (Yamauchi *et al.*, 1992) is found to be active in growing thermophiles and hyperthermophiles (Yamauchi *et al.*, 1992; Matsumoto *et al.*, 1999) at rates that exceed the racemization rate of aspartic acid. Because known aspartate racemase preferentially converts L-aspartic acid to D-aspartic acid (Yamauchi *et al.*, 1992), however, it will likely not mitigate increasing D/L values for free aspartic acid, forcing metabolizing subsurface micro-organisms to regenerate L-aspartic acid for the proteins that are needed to replace those damaged by aspartic acid racemization.

The low D/L values we have discovered for the protein contained with the planktonic microbial cells indicate that on average they are *living* micro-organisms. For expired micro-organisms, the proteins and cell wall peptides denature and enter the extracellular amino acid pool not sampled by our filter. There, they continue to racemize at

rates that are 2–4 times slower than the *in vivo* rate (Bada, 1972; Bada & Schroeder, 1975). The amino acids associated with the cell wall constituents of micro-organisms, for example peptidoglycan, have a higher D/L than those of proteins and are more recalcitrant within their polymer matrix. As a result, prokaryotic cell wall amino acids are hypothesized to comprise the majority of the bulk amino acid pool in seafloor sediments (Grutters *et al.*, 2002; Lomstein *et al.*, 2012), becoming a part of the extracellular bacterial 'necromass' of Parkes *et al.* (1993) that dwarfs the *living* bacterial biomass by at least two orders of magnitude. The similarity between the cell counts and the protein concentrations in this study and that of Takano *et al.* (2003), however, suggests that no comparably huge bacterial 'necromass' is suspended in the fracture water of terrestrial rocks.

Depurination rates

The temperature dependency of *in vivo* aspartic acid racemization rate (Masters *et al.*, 1977) closely matches the *in vitro* rate of nucleic acid depurination (Lindahl & Nyberg, 1972), which creates apurinic sites in DNA and RNA that would ultimately lead to nucleic acid fragmentation. In ancient samples where aspartic acid D/L values exceed 0.08, the DNA fragments are <100 bp and this may in part reflect the formation of apurinic sites (Poinar *et al.*, 1996). The time required for racemization of 2% of the L-aspartic acid to D-aspartic acid (solid black line in Fig. 1A) overlaps within error of the time required for depurination of 1 purine base in 100 purine bases (solid gray lines in Fig. 1A). The same DNA base excision repair (BER) pathway is used by thermophiles and mesophiles to repair apurinic sites, but it has been shown recently that the endonuclease IV repair protein that is responsible for DNA repair in thermophiles is stable to 90 °C, 20 °C higher than the same protein in mesophiles (Haas *et al.*, 1999). The BER pathway and constitutive proteins also appear to operate at rates exceeding the *in vivo* DNA depurination rate (Kaboev *et al.*, 1985). Nonetheless, if the cellular protein generation rates cannot keep pace with *in vivo* aspartic acid racemization and DNA depurination, then key metabolic and DNA repair pathways will fail, proteins and DNA will degrade, and the micro-organism will expire (Bada, 1984).

The *in vitro* experimental parameters for DNA depurination (Lindahl & Nyberg, 1972) predict that 1% depurination of the DNA would occur in 0.6 years at the *in situ* temperature of MP104. The *in vitro* depurination rates are affected by pH, however, and for the *in situ* pH of 8.5 for the MP104 fracture water, 1% depurination of the DNA would require ~2 years (gray dashed line in Fig. 1A), which is comparable to the maximum cellular protein turnover time. The DNA extracted from the same filter by Chivian *et al.* (2008) used in the amino acid analyses yielded heavy molecular weight DNA, at least 12 kb in size (Fig. 2 in the Appendix S1), indicating that the genomic DNA was largely intact and not depurinated at the 1% level. Chivian *et al.* (2008) also reported that the heterogeneity in the DNA sequences as measured by single-nucleotide polymorphisms was quite low, yielding only 32 positions with a SNP recorded more than once. This apparent paucity of mutations in multiple copies of the 2.35-Mb genome from a total population of $\sim 10^{11}$ cells suggested to them that either a recent, environmentally imposed selective sweep had occurred or some highly restrictive environmental constraint minimized neutral drift.

The high quality of the DNA and low SNP in the presence of a short turnover time for cellular protein can be interpreted in one of the following ways: (i) total cellular turnover, both amino acids and DNA, has occurred over the course of a year or two in this deep fracture under conditions that selected for *Ca. D. audaxviator* or (ii) the DNA turnover has occurred very slowly, perhaps on the time scale of thousands of years, but the BER pathway is very active and the repair proteins possess very high fidelity correcting for any mutations.

Minimum metabolic rates from anabolic rates

Sample MP104 possesses the best evidence for the dominance of autotrophic sulfate reduction (Lin *et al.*, 2006; Chivian *et al.*, 2008). The cellular amino acid turnover time, $t_{\max_{Asp}}$, of 1.7–1.8 (−0.3/+0.4) years determined for the MP104 sample is less than the 45- to 300-year cellular turnover times estimated for the same fracture water by Lin *et al.* (2006). If the geochemically estimated cellular turnover times were accurate, then the D/L ratio of aspartic acid would have been at least 0.7 (thin solid line in Fig. 1A) and would have indicated that almost all of the observed cells were inactive at the time of sampling. The total cellular amino acid concentration of 47.9 ng L^{-1}/ 0.7 = 68 ng L^{-1} indicates a minimum protein generation rate of 38–40 ng L^{-1} $year^{-1}$. Given that 99% of the 16S rRNA gene sequences from this fracture water were comprised of a chemolithoautotrophic SRB, *Ca. D. audaxviator*, the application of equation (13) to estimate the metabolic rate for autotrophic sulfate reduction is justified. Approximately 9.1×10^{-2} moles of ATP is required to generate one gram of protein from CO_2 (Stouthamer, 1979), and 1.3 moles of ATP is produced for every mole of sulfate reduced by H_2 (Jin & Bethke, 2005). The anabolic rate therefore would require a minimum sulfate reduction rate of 2.6–2.8 (+1.0/−0.8) nM $year^{-1}$ (Table 6), which is greater than the 0.2–1.5 nM $year^{-1}$ estimated by Lin *et al.* (2006). This rate is also more than the 0.2–0.45 nM $year^{-1}$ sulfate production rate predicted for radiolytic oxidation of pyrite in the Witwatersrand and

Ventersdorp Supergroups, respectively (Lin *et al.*, 2005). The likely explanation for the higher-than-expected geochemical flux of H_2 and sulfate may lie in a more recently discovered release of H_2 during fracturing of the rock formations with mining activity (Lippmann-Pipke *et al.*, 2011a). Phylogenetic analyses and sulfur isotopic data suggest that the other deeper fracture water samples are dominated by SRB activity. The highest estimated minimum metabolic rate, 20 nM $year^{-1}$, was for KL441 (Table 6), which has a much younger noble gas age than the other deep and more saline fracture water (Table 1), suggesting that a greater fluid flux may be supporting a greater biomass. The high cellular concentrations, high temperatures, and low D/L values for the aspartic acid observed at Toyoha mine also require very high metabolic rates, presumably sustained by the current geothermal activity of this deposit (Ohta, 1991).

Cellular inactivation, maintenance, and aspartic acid racemization

The low D_0/L_0 values of aspartic acid in the planktonic micro-organisms from the deep fractures of South Africa indicate that they are actively replacing their cellular proteins. If the replacement of cellular proteins compromised by the racemization of aspartic acid were the primary drain on ATP consumption in micro-organisms in maintenance mode, then the t_{Asp} estimates of cellular protein turnover times should coincide with or be less than the cellular inactivation rates in survival studies, that is, when viable populations are declining due to irreversible inactivation of cellular enzymes (Morita, 1997).

Takahata *et al.* (2001) performed starvation survival experiments at 80 °C and 90 °C on *Thermococcus* strains isolated from deep-sea hydrothermal vents and oil reservoirs. The starvation experiments were performed in sterilized seawater and oil formation water using cells grown on yeast extract and monitored for 60 days. Takahata *et al.* (2001) reported survival time half-lives, mathematically equivalent to t_{Asp}, ranging from <1 day to 30 days (gray triangles in Fig. 1B). Takahata *et al.* (2001) also reported that the subsurface *Thermococcus* strains required L-amino acids in their media in order to grow at their optimum temperature, which would significantly reduce their ATP requirement (Stouthamer, 1979).

Takai *et al.* (2008) performed starvation survival experiments at 121 °C and 130 °C at 0.4 and 30 MPa on methanogen *Methanopyrus kandleri* strain 116. They reported survival half-lives ranging from 0.7 to 2 h at 121 °C and from 0.2 to 0.3 h at 130 °C with high-pressure survival experiments yielding longer half-lives (open triangles in Fig. 1B).

Boone *et al.* (1995) performed starvation survival experiments at 50 °C and 70 °C on the obligate anaerobic Fe^{3+}-reducing *Bacillus infernus*. They found minimal survival times of 52 and 27 days for 50 °C and 70 °C, respectively, but the organism may have sporulated, and hence, these estimates are treated as minimum estimates (inverted gray triangles in Fig. 1B). The t_{Asp} values calculated using equation (7) and D/L values of aspartic acid ranging from 0.02 to 0.2 straddle the range of half-lives observed in these starvation survival experiments (dashed dark line in Fig. 1B).

Within non-growing cells, protein degradation and synthesis (i.e. turnover) continue at rates lower than those in growing cells and the total cellular protein per cell mass has been observed to increase as other constituents are degraded (Kjelleberg *et al.*, 1987). Protein turnover times, however, are thought to remain significantly shorter than cellular doubling times given that the energetic cost of complete replication of genomic DNA and lipid membranes exceeds that of protein production (Stouthamer, 1979; Morita, 1997). The t_{Asp} estimates of cellular protein turnover times therefore should coincide with that derived from cells in maintenance mode, that is, when cells are maintaining a constant viable population size (Morita, 1997). Maintenance mode is modeled experimentally from chemostat growth experiments at low dilution rates (Tijhuis *et al.*, 1993) or determined directly by recycling fermenters (retentostats), although slow or cryptic growth likely occurs even for retentostats (Arbige & Chesbro, 1982) in which case the t_{Asp} estimates will be greater than the cellular protein turnover times, t_{cell}, derived from these experiments.

The t_{cell} values measured in chemostats (Habicht *et al.*, 2005; VerEecke *et al.*, 2012) and in retentostats (Davidson *et al.*, 2009) for thermophilic organisms ranged from <1 day to 6 days (inverted open and dotted triangles in Fig. 1B), whereas for mesophilic organisms the cellular protein turnover times measured in chemostats (Peters *et al.*, 1998; Scholten & Conrad, 2000) (inverted solid and dotted triangles in Fig. 1B) and retentostats (Colwell *et al.*, 2008) (solid squares with crosses in Fig. 1B) ranged from 10 to 300 days. At thermophilic temperatures, the t_{cell} values are ~10× shorter than the t_{Asp} values calculated for a D/L value of 0.02 and ~100× shorter than the t_{Asp} values at mesophilic temperatures (Fig. 1B). The difference between the t_{cell} and t_{Asp} values may be due to (i) cryptic growth in the experiments, (ii) the cells that are maintaining their D/L of aspartic acid at a level significantly less than 0.02, and/or (iii) other mechanisms that are responsible for irreversible enzyme inactivation under chemostat or retentostat conditions.

Further evidence for high specific catabolic rates for thermophiles is suggested by $^{35}SO_4$-measured *in situ* sulfate reduction rates within hot spring sediments in Yellowstone National Park (Fishbain *et al.*, 2003). The cellular protein turnover times for this study were based upon

$^{35}SO_4$-measured sulfate reduction rates (moles SO_4 cm^{-3} h^{-1}), an assumed sediment density of 1.5 g cm^{-3}, phospholipid concentrations (nmol g^{-1}), a conversion factor of 2.5×10^4 cells (pmol of phospholipid)$^{-1}$, 1.3 moles of ATP per mole of sulfate reduced, 2.05×10^{-4} of ATP per gram of protein produced, and 156 fg C $cell^{-1}$. With these assumptions and utilizing equation (1), the estimated SRB cellular protein turnover times in these sediments whose *in situ* temperatures ranged from 80 to 91 °C were 0.2 to 2 days (gray diamonds in Fig. 1B) comparable to the t_{Asp} values calculated for a D/L value of 0.02.

All of the experimental constraints listed above suggest that a D/L value of aspartic acid ranging from 0.02 to <0.2 defines the boundary between *living* thermophiles and hyperthermophiles and dead ones.

Other estimates of maintenance and aspartic acid racemization rates

For comparison, we have plotted (dashed line in Fig. 1B) the maintenance energy demand, kJ (Cmol of biomass)$^{-1}$ h^{-1}, derived by Tijhuis *et al.* (1993), converted to cellular turnover times using the energy-to-biomass ratio, kJ (Cmol of biomass)$^{-1}$, derived by McCollom & Amend (2005) for anaerobes. As has been noted before by Hoehler (2004), Scholten & Conrad (2000), and Davidson *et al.* (2009), the maintenance energy demand derived by Tijhuis *et al.* (1993) from chemostat experiments exceeds that determined in the more recent experiments of Scholten & Conrad (2000), Colwell *et al.* (2008), and Davidson *et al.* (2009) by 2–3 orders of magnitude, with the disparity increasing with decreasing temperature. This discrepancy may reflect differences in the maintenance energy demand for slow-growing vs. truly non-growing bacteria (Kjelleberg *et al.*, 1987).

Brinton *et al.* (2002) determined aspartic acid racemization rates from experiments in which permafrost sediment samples were heated to temperatures ranging from 102 to 148 °C. Given the high temperatures used in these experiments, the temperature dependence of the proton permeability of cytoplasmic membranes (van de Vossenberg *et al.*, 1995) and of protein denaturation of a cell's proteome (Dill *et al.*, 2011), the aspartic acid racemization rate should represent that of free amino acids in a mineral/water matrix. For a D/L ratio of 0.02, the kinetic parameters of Brinton *et al.* (2002) yield t_{Asp} values (thin solid line in Fig. 1B) that are identical within error of those determined from the *in vivo* aspartic acid racemization rates for temperatures of 75–90 °C. With decreasing temperatures, the trend in t_{Asp} values predicted by the Brinton *et al.* (2002) parameters is subparallel to the cellular protein turnover times derived from chemostat experiments but departs from the trend set by the *in vivo* aspartic acid racemization rates. At 25 °C, the aspartic acid racemization rate predicted by the Brinton *et al.*'s (2002) parameters is 20 times that predicted by the experimental data of Bada (1972) for free amino acids at neutral pH and 10 times that predicted by the *in vivo* aspartic acid racemization rate. When analyzing the D/L ratio of aspartic acid directly from sediments, the choice of the aspartic acid racemization parameters therefore will have a significant impact on the deduced protein turnover times at the low temperatures of permafrost deposits and of seafloor sediments (Fig. 1B), for example the calculations of Lomstein *et al.* (2012) who utilized the parameters of Bada (1982).

The cellular turnover times estimated by Lomstein *et al.* (2012) (open diamond in Fig. 1A) are somewhat shorter than the protein turnover times required to maintain an aspartic acid D/L ratio of 0.02 at temperatures of 9–15 °C and coincide with the turnover time predicted for a depurination of 1% at the same temperatures (gray solid line in Fig. 1A), but they are more than the protein turnover times required to maintain an aspartic acid D/L ratio of 0.02 when the racemization rates of Brinton *et al.* (2002) are utilized. The cellular doubling times estimated by Schippers *et al.* (2005), however, are much shorter than those estimated by either racemization rate and appear to lie on an extension of the chemostat/retentostat trend as a function of temperature (Fig. 1A,B). The determination of cellular turnover times in subseafloor sediments is further obfuscated by the fact that the amino acid pool in the mixing layer of the seafloor is predominantly comprised of cell wall proteins, which have greater D/L values than the other cellular proteins. These cell wall proteins are subsequently buried and mixed with the amino acid pool of *living* micro-organisms. Another complication is the large fraction of spores that are present and were assumed by Lomstein *et al.* (2012) to be part of the *living* bacterial pool. Lomstein *et al.* (2012), however, used the D/L ratio of aspartic acid from vegetative cells, not cell walls and not spores, to correct for the D/L values of aspartic acid in the sediments. Their protein doubling times for the *living* micro-organisms therefore could be significantly overestimated. Resolution of the true cellular protein doubling time of *living* micro-organisms in subseafloor sediments should be feasible in future studies, however, using a new counting method developed by Kallmeyer *et al.* (2008), which removes cells from the sediments.

Constraints on the depth and mass of the *living* subsurface biosphere

The deep subsurface biosphere may contain the majority of the Earth's prokaryotes, comprising ~37–48% of its total *living* biomass (Whitman *et al.*, 1998), and may play a significant role in the cycling of carbon on Earth (Colwell & D'Hondt, 2013). The exact size of the subsurface

biosphere, however, is difficult to constrain because of limited access, and recent data suggest that the marine subsurface biosphere comprises far less biomass than previously believed (Kallmeyer *et al.*, 2012), but does this diminish its importance in cycling carbon as well? Certainly with increasing depth and temperature, the subsurface biosphere must diminish, but the upper temperature limit for subsurface life is not well established. The apparent paucity of biodegraded oil in reservoirs with formation temperatures >80 °C (Connan, 1984) has been interpreted as indicating upper temperature bounds for active subsurface ecosystems in low-porosity and hydraulically tight-fractured rock (Larter *et al.*, 2003). A hyperthermophilic methanogen capable of growing at temperatures up to 122 °C has been isolated from a deep-sea hydrothermal vent (Takai *et al.*, 2008), but does the high-energy flux and high-porosity of hot springs or hydrothermal vents explain the occurrence of hyperthermophiles? Röling *et al.* (2003) reported that for oil reservoirs with temperatures >80 °C, the isolation of hyperthermophilic bacteria or archaea was extremely rare. Nevertheless, hyperthermophilic *Thermococcus* strains have been isolated from oil field formation water from western Siberia (Miroshnichenko *et al.*, 2001), the Sea of Japan (Takahata *et al.*, 2001), and Paris Basin (L'Haridon *et al.*, 1995), where *in situ* temperatures were less than their optimum growth temperatures of 78–85 °C. Species belonging to *Archaeaoglobus*, *Pyrococcus*, and *Thermococcus* with optimum growth temperatures of 80–92 °C were isolated from a sea water-flooded petroleum reservoir, but their indigenousness was questioned by Stetter *et al.* (1993). The presence of hyperthermophiles, but absence of *in situ* hyperthermophilic activity, led Röling *et al.* (2003) to suggest that at temperatures >80 °C, cells require rapid anabolic rates in order to replace cellular constituents.

In the Witwatersrand Basin, the cellular concentrations range from $10^{6–7}$ cells L^{-1} and do not diminish with depth down to 3.5 km (Onstott *et al.*, 2010). Depths corresponding to 85 °C occur at ~6–7 km. The t_{Asp} at this temperature would be a couple of days in order to keep pace with *in vivo* racemization (Fig. 1); otherwise, enzymatic activity would diminish to the point that the cells' enzymes would become irreversibly inactivated and the cells would perish. For an SRB-dominated community like that of MP104 at 85 °C and the observed D/L-aspartic acid ratio of 0.04, the t_{Asp} would be ~4 days. A cellular concentration of 10^7 cells L^{-1} would require a sulfate reduction rate of ~400 nM $year^{-1}$, or the protein concentration would have to be 0.3 ng L^{-1} (~10^4 cells L^{-1}) for a bulk sulfate reduction rate of 2.6 nM $year^{-1}$. Thus, if the energy flux at ~6 km depth were the same as that at 3 km depth, then the cellular concentrations would have to decline by three orders of magnitude. At a depth of 10 km, where the temperature is 120 °C, the t_{Asp} would be 1 h, a 2.6 nM $year^{-1}$ bulk sulfate reduction rate could only sustain $10^{1–2}$ cells L^{-1}. In all likelihood, the energy fluxes would decline with increasing depth as increasing lithostatic pressure would reduce fracture permeability leading to a rapid attenuation of the *living* biomass abundance.

This analysis suggests that the anabolic requirement to turn over proteins on an almost daily basis and the catabolic requirement imposed would severely limit the concentration of *living* subsurface micro-organisms and this may explain an apparent absence of biodegradation in petroleum-bearing strata at temperatures of 85 °C (Wilhelms *et al.*, 2001). This analysis also suggests that in deep subsurface environments where accessibility to carbon substrates is high, the carbon cycling will also be very high because of the anabolic requirements. High-energy flux environments such as thermal springs and deep-sea hydrothermal vents may be able to support such rapid cellular turnover, but low-porosity subsurface sediment and hydraulically tight, fractured rock environments will not.

CONCLUSIONS

If the deep subsurface is energy-limited, then existence of a *living* subsurface biosphere comparable in size to that of the surface biosphere is contingent on the ability of microorganisms to survive within the required anabolic energy demands over extremely long time scales. The smaller this anabolic energy demand, the larger the *living* subsurface biosphere can be. In order to significantly improve our estimate of the global *living* subsurface biosphere, we either need a means of directly measuring the *in situ* anabolic rate or a much better understanding of the environmental controls on the anabolic energy demand or preferably both. The amount of energy required to repair protein damage due to racemization and DNA damage due to depurination has been proposed to constrain the minimum energy requirement for microbial survival (Morita, 1997; Hoehler, 2004), and the rates for these processes are strongly temperature dependent (Price & Sowers, 2004).

In this study, we found that the D/L values of aspartic acid of intact planktonic cells collected from 3-km-deep fractures in South Africa revealed that the cells exhibit little racemization, indicating that the bulk of the cells are *living*. Application of the rate parameters for racemization provided us a means of directly determining *in situ* anabolic rates independent of assumptions about *living* biomass concentrations, and this approach yielded surprisingly short cellular protein turnover times of 1–2 years for the deepest, hottest samples. We also found that a D/L value of aspartic acid that ranges from 0.02 to 0.2 yields protein turnover times that are comparable to experimentally determined death rates and *in situ* protein turnover times for thermophiles and hyperthermophiles. The high

catabolic demand required to keep the D/L value of aspartic acid below 0.02–0.2 constrains the abundance of *living* cells at high temperatures and may explain an apparent paucity of biodegradation of oil in reservoirs where the temperatures are greater than 85 °C. Amino acid analyses of the cellular proteins of planktonic communities filtered from oil field formation water could provide direct tests of this hypothesis. If the hypothesis that aspartic acid racemization is the principal maintenance energy demand at thermophilic temperatures is correct, then it may be possible to more accurately estimate the global *living* subsurface biosphere from heat flow measurements, geochemistry, and fluid flux constraints. Determination of the D/L value of aspartic acid in thermophiles and hyperthermophiles living in retentostats could improve the accuracy of this approach. When combined with proteomic analyses, which potentially identifies the principal metabolic pathways being expressed by the micro-organisms (Ram *et al.*, 2005), the connection between the anabolic rate and metabolic rate could also be better constrained, thereby improving biogeochemical models of the deep subsurface biosphere.

ACKNOWLEDGMENTS

We would like to thank Gold Fields Ltd., Dawie Nell, and the managers and staff of Driefontein Au mine; Tim Hewitt and the managers and staff of Kloof; and Anglogold Ashanti Ltd., David Kershaw, and the managers and staff of Mponeng Au mine for their logistical support during the collection of the samples for this study. The laboratory analyses were completed at Scripps Institution of Oceanography, University of California at San Diego, and Goddard Space Flight Center, Greenbelt, Maryland. We thank David Culley of Pacific Northwest National Laboratory for providing the gel image of the MP104 DNA extract. This work was supported in part by an appointment to the NASA Postdoctoral Program at the Jet Propulsion Laboratory, California Institute of Technology, administered by Oak Ridge Associated Universities through a contract with NASA. T.C.O. acknowledges the support of NASA Astrobiology Institute through award NNA04CC03A to the IP-TAI Team and Professor L.M. Pratt of Indiana University and to NSF through award EAR-0948659. T.L.K. acknowledges support from NSF (EAR-0948335 and EAR-0948335). We are grateful to two anonymous reviewers whose comments significantly improved the quality of the final manuscript.

REFERENCES

Arbige M, Chesbro W (1982) relA and related loci are growth rate determinants for *Escherichia coli* in a recycling fermenter. *Journal of General Microbiology* **128**, 693–703.

Atlas RM (1993) *Handbook of Microbiological Media*. CRC Press, Boca Raton, FL.

Aubrey AD (2008) Amino acid biosignatures: implications for the detection of extinct or extant microbial communities on Mars. Ph.D. Thesis, Department of Oceanography. University of California, San Diego, p. 228.

Bada JL (1972) Kinetics of racemization of amino acids as a function of pH. *Journal of the American Chemical Society* **94**, 1371–1373.

Bada JL (1982) Racemization of amino acids in nature. *Interdisciplinary Science Reviews* **7**, 30–46.

Bada JL (1984) *In vivo* racemization in mammalian proteins. *Methods in Enzymology* **106**, 98–115.

Bada JL, Schroeder RA (1975) Amino acid racemization reactions and their geochemical implications. *Naturwissenschaften* **62**, 71–79.

Bada JL, Wang XYS, Hamilton H (1999) Preservation of key biomolecules in the fossil record: current knowledge and future challenges. *Philosophical Transactions of the Royal Society of London. Series B, Biological Sciences* **354**, 77–86.

Boone DR, Liu Y, Zhao Z-J, Balkwill DL, Drake GR, Stevens TO, Aldrich HC (1995) *Bacillus infernus* sp. nov., an Fe(II1)- and Mn(1V)-Reducing Anaerobe from the Deep Terrestrial Subsurface. *International Journal of Systematic Bacteriology* **45**, 441–448.

Borgonie G, García-Moyano A, Litthauer D, Bert W, Bester A, Heerden Ev, Onstott TC (2011) Nematoda from the terrestrial deep subsurface of South Africa. *Nature* **474**, 79–82.

Brinton KLF, Tsapin AI, Gilichinsky D, McDonald GD (2002) Aspartic acid racemization and age–depth relationships for organic carbon in Siberian permafrost. *Astrobiology* **2**, 77–82.

Butlin KR, Adams ME, Thomas M (1949) The isolation and cultivation of sulfate-reducing bacteria. *Microbiology* **3**, 46–59.

Chivian D, Alm E, Brodie E, Culley D, Dehal P, DeSantis T, Gihring T, Lapidus A, Lin L-H, Lowry S, Moser D, Richardson P, Southam G, Wanger G, Pratt L, Andersen G, Hazen T, Brockman F, Arkin A, Onstott T (2008) Environmental genomics reveals a single species ecosystem deep within the Earth. *Science* **322**, 275–278.

Colwell FS, D'Hondt S (2013) Nature and Extent of the Deep Biosphere. In *Carbon in Earth*. (eds Hazen RM, Jones AP, Baross JA). Mineralogical Society of America, Chantilly, VA, pp. 547–566.

Colwell FS, Boyd S, Delwiche ME, Reed DW, Phelps TJ, Newby DT (2008) Estimates of biogenic methane production rates in deep marine sediments at hydrate ridge, cascadia margin. *Applied and Environment Microbiology* **74**, 3444–3452.

Connan J (1984) Biodegradation of crude oils in reservoirs. In *Advances in Petroleum Geochemistry*. (eds Brooks J, Welte DH). Academic Press, London, pp. 299–330.

Davidson MM, Bisher ME, Pratt LM, Fong J, Southam G, Pfiffner SM, Reches Z, Onstott TC (2009) Sulfur isotope enrichment during maintenance metabolism in the thermophilic sulfate-reducing bacterium Desulfotomaculum putei. *Applied and Environment Microbiology* **75**, 5621–5630.

D'Hondt S, Rutherford S, Spivack AJ (2002) Metabolic activity of subsurface life in deep-sea sediments. *Science* **295**, 2067–2070.

Dill KA, Ghosh K, Schmit JD (2011) Physical limits of cells and proteomes. *Proceedings of the National Academy of Sciences of the USA* **108**, 17876–17882.

Fishbain S, Dillon J, Gough HL, Stahl DA (2003) Linkage of high rates of sulfate reduction in Yellowstone hot springs to unique sequence types in the dissimilatory sulfate respiration

pathway. *Applied and Environmental Microbiology* **69**, 3663–3667.
Geiger T, Clarke S (1987) Deamidation, isomerization, and racemization at Asparaginyl and Aspartyl residues in peptides. *The Journal of Biological Chemistry* **262**, 785–794.
Gihring TM, Moser DP, Lin L-H, Davidson MM, Onstott TC, Morgan L, Milleson M, Kieft T, Trimarco E, Balkwill DL, Dollhopf M (2006) The distribution of microbial taxa in the subsurface water of the Kalahari Shield, South Africa. *Geomicrobiology Journal* **23**, 415–430.
Glavin DP, Schubert M, Botta O, Kminek G, Bada JL (2001) Detecting pyrolysis products from bacteria on Mars. *Earth and Planetary Science Letters* **185**, 1–5.
Glavin DP, Dworkin JP, Aubrey A, Botta O, Doty JH III, Martins Z, Bada JL (2006) Amino acid analyses of Antarctic CM2 meteorites using liquid chromatography-time of flight-mass spectrometry. *Meteoritics & Planetary Science* **41**, 889–902.
Glavin DP, Aubrey AD, Callahan MP, Dworkin JP, Elsila JE, Parker ET, Bada JL, Jennisken P, Shaddad MH (2010) Extraterrestrial amino acids in the Almahata Sitta meteorite. *Meteoritics & Planetary Science* **45**, 1695–1709.
Greaves RB, Warwicker J (2007) Mechanisms for stabilisation and the maintenance of solubility in proteins from thermophiles. *BMC Structural Biology* **7**, 18.
Grutters M, van Raaphorst W, Epping E, Helder W, de Leeuw JW, Glavin DP, Bada J (2002) Preservation of amino acids from *in situ*–produced bacterial cell wall peptidoglycans in northeastern Atlantic continental margin sediments. *Limnology and Oceanography* **47**, 1521–1524.
Haas BJ, Sandigursky M, Tainer JA, Franklin WA, Cunningham RP (1999) Purification and characterization of *Thermotoga maritima* endonuclease IV, a thermostable apurinic/apyrimidinic endonuclease and 39-repair diesterase. *Journal of Bacteriology* **181**, 2834–2839.
Habicht KS, Canfield DE (1996) Sulphur isotope fractionation in modern microbial mats and the evolution of the sulphur cycle. *Nature* **382**, 342–343.
Habicht KS, Salling L, Thamdrup B, Canfield DE (2005) Effect of low sulfate concentrations on lactate oxidation and isotope fractionation during sulfate reduction by archaeoglobus fulgidus strain Z†. *Applied and Environment Microbiology* **71**, 3770–3777.
Hayashi R, Kameda I (1980) Racemization of amino acid residues during alkali-treatment of protein and its adverse effect on pepsin digestibility. *Agricultural Biological Chemistry* **44**, 891–895.
Heijnen JJ, van Dieken JP (1992) In search of a thermodynamic description of biomass yields for the chemotrophic growth of microorganisms. *Biotechnology and Bioengineering* **39**, 833–858.
Hoehler TM (2004) Biological energy requirements as quantitative boundary conditions for life in the subsurface. *Geobiology* **2**, 205–215.
Jin Q, Bethke CM (2005) Predicting the rate of microbial respiration in geochemical environments. *Geochimica et Cosmochimica Acta* **69**, 1133–1143.
Kaboev OK, Luchkina LA, Kuziakin TI (1985) Apurinic and apyrimidinic DNA endonuclease of extremely thermophilic *Thermothrix thiopara*. *Journal of Bacteriology* **164**, 878–881.
Kaiser K, Benner R (2005) Hydrolysis-induced racemization of amino acids. *Limnology and Oceanography: Methods* **3**, 318–325.
Kallmeyer J, Smith D, D'Hondt S, Spivack A (2008) New cell extraction procedure applied to deep subsurface sediments. *Limnology and Oceanography: Methods* **6**, 236–245.
Kallmeyer J, Pockalny R, Adhikari RR, Smith DC, D'Hondt S (2012) Global distribution of microbial abundance and biomass in subseafloor sediment. *Proceedings of the National Academy of Sciences of the USA* **109**, 16213–16216.
Kandler O, Konig H (1978) Chemical composition of the peptidoglycan-free cell walls of methanogenic bacteria. *Archives of Microbiology* **118**, 141–152.
Kieft T, McCuddy S, Onstott T, Davidson M, Lin L-H, Mislowack B, Pratt L, Boice E, Sherwood Lollar B, Lippmann-Pipke J, Pfiffner S, Phelps T, Gihring T, Moser D, van Heerden A (2005) Geochemically generated, energy-rich substrates and indigenous microorganisms in deep, ancient groundwater. *Geomicrobiology Journal* **22**, 325–355.
Kjelleberg S, Hermansson M, Mårdén P, Jones GW (1987) The transient phase between growth and nongrowth of heterotrophic bacteria, with emphasis on the marine environment. *Annual Review of Microbiology* **41**, 25–49.
Larter S, Wilhelms A, Head I, Koopmans M, Aplin A, Primio RD, Zwach C, Erdmann M, Telnaes N (2003) The controls on the composition of biodegraded oils in the deep subsurface—part 1: biodegradation rates in petroleum reservoirs. *Organic Geochemistry* **34**, 601–613.
L'Haridon S, Reysenbach A-L, Glenat P, Prieur D, Jeanton C (1995) Hot subterranean biosphere in a continental oil reservoir. *Nature* **377**, 223–224.
Li J, Brill TB (2003) Spectroscopy of hydrothermal reactions part 26: kinetics of decarboxylation of aliphatic amino acids and comparison with the rates of racemization. *International Journal of Chemical Kinetics* **35**, 602–610.
Lin LH, Hall J, Lippmann-Pipke J, Ward JA, Lollar BS, DeFlaun M, Rothmel R, Moser D, Gihring TM, Mislowack B, Onstott TC (2005) Radiolytic H_2 in continental crust: nuclear power for deep subsurface microbial communities. *Geochemistry Geophysics Geosystems* **6**, 1–13.
Lin LH, Wang P-L, Rumble D, Lippmann-Pipke J, Boice E, Pratt LM, Sherwood Lollar B, Brodie E, Hazen T, Andersen G, DeSantis T, Moser DP, Kershaw D, Onstott TC (2006) Long term biosustainability in a high energy, low diversity crustal biome. *Science* **314**, 479–482.
Lindahl T, Nyberg B (1972) Rate of depurination of native deoxyribonucleic acid. *Biochemistry* **11**, 3610–3618.
Lippmann J, Stute M, Torgersen T, Moser DP, Hall J, Lin L, Borcsik M, Bellamy RES, Onstott TC (2003) Dating ultra-deep mine waters with noble gases and ^{36}Cl, Witwatersrand Basin, South Africa. *Geochimica et Cosmochimica Acta* **67**, 4597–4619.
Lippmann-Pipke J, Erzinger J, Zimmer M, Kujawa C, Boettcher M, Heerden EV, Bester A, Moller H, Stroncik NA, Reches Z (2011a) Geogas transport in fractured hard rock – Correlations with mining seismicity at 3.54 km depth, TauTona gold mine, South Africa. *Applied Geochemistry* **26**, 2134–2146.
Lippmann-Pipke J, Sherwood Lollar B, Neidermann S, Stroncik N, Naumann R, VanHeerden E, Onstott TC (2011b) Neon identifies two billion year old fluid component in Kaapvaal Craton. *Chemical Geology* **282**, 287–296.
Lomstein BA, Langerhuus AT, D'Hondt S, Jørgensen BB, Spivack AJ (2012) Endospore abundance, microbial growth and necromass turnover in deep sub-seafloor sediment. *Nature* **484**, 101–104.
Masters PM, Bada JL, Zigler JS (1977) Aspartic acid racemisation in the human lens during ageing and in cataract formation. *Nature* **268**, 71–73.
Matsumoto M, Homma H, Long Z, Imai K, Iida T, Maruyama T, Aikwa Y, Endo I, Yohda M (1999) Occurrence of free D-amino

acids and aspartate racemases in hyperthermophilic archaea. *Journal of Bacteriology* **181**, 6560–6563.
McCollom TM, Amend JP (2005) A thermodynamic assessment of energy requirements for biomass synthesis by chemolithoautotrophic micro-organisms in oxic and anoxic environments. *Geobiology* **3**, 135–144.
Miroshnichenko ML, Hippe H, Stackebrandt E, Kostrikina NA, Chernyh NA, Jeanthon C, Nazina TN, Belyaev SS, Bonch-Osmolovskaya EA (2001) Isolation and characterization of *Thermococcus sibiricus* sp. nov. from a Western Siberia high-temperature oil reservoir. *Extremophiles* **5**, 85–91.
Morita R (1997) *Bacteria in Oligotrophic Environments: Starvation-Survival Lifestyle*. Chapman and Hall, New York.
Moser DP, Gihring T, Fredrickson JK, Brockman FJ, Balkwill D, Dollhopf ME, Sherwood-Lollar B, Pratt LM, Boice E, Southam G, Wanger G, Welty AT, Baker BJ, Onstott TC (2005) *Desulfotomaculum* spp. and *Methanobacterium* spp. Dominate 4–5 km deep fault. *Applied and Environmental Microbiology* **71**, 8773–8783.
Ohta E (1991) Polymetallic mineralization at the Toyoha mine, Hokkaido, Japan. *Mining Geology* **41**, 279–295.
Onstott TC, Lin L-H, Davidson M, Mislowack B, Borcsik M, Hall J, Slater GF, Ward J, Sherwood Lollar B, Lippmann-Pipke J, Boice E, Pratt LM, Pfiffner SM, Moser DP, Gihring T, Kieft TL, Phelps TJ, van Heerden E, Litthaur D, DeFlaun M, Rothmel R (2006) The origin and age of biogeochemical trends in deep fracture water of the Witwatersrand Basin, South Africa. *Geomicrobiology Journal* **23**, 369–414.
Onstott TC, van Heerden E, Murdoch L (2010) Microbial life in the depths of the earth. *Géosciences, la revue du BRGM pour une Terre Durable* **11**, 52–59.
Parkes RJ, Cragg BA, Getliff JM, Harvey SM, Fry JC, Lewis CA, Rowland SJ (1993) A quantitative study of microbial decomposition of biopolymers in recent sediments from the Peru Margin. *Marine Geology* **113**, 55–66.
Peters V, Janssen PH, Conrad R (1998) Efficiency of hydrogen utilization during unitrophic and mixotrophic growth of Acetobacterium woodii on hydrogen and lactate in the chemostat. *FEMS Microbiology Ecology* **26**, 317–324.
Pfiffner SM, Cantu JM, Smithgall A, Peacock AD, White DC, Moser DP, Onstott TC, van Heerden E (2006) Deep subsurface microbial biomass and community structure in Witwatersrand Basin mines. *Geomicrobiology Journal* **23**, 431–442.
Phelps TJ, Murphy EM, Pfiffner SM, White DC (1994) Comparison between geochemical and biological estimates of subsurface microbial activities. *Microbial Ecology* **28**, 335–349.
Poinar HN, Höss M, Bada JL, Pääbo S (1996) Amino acid racemization and the preservation of ancient DNA. *Science* **272**, 864–866.
Price PB, Sowers T (2004) Temperature dependence of metabolic rates for microbial growth, maintenance, and survival. *Proceedings of the National Academy of Science of the USA* **101**, 4631–4646.
Ram R, VerBerkmoes N, Thelen M, Tyson G, Baker B, Blake R II, Manesh SM, Hettich R, Banfield J (2005) Community proteomics identifies key activities in a natural microbial biofilm. *Science* **308**, 1915–1920.
Röling WFM, Head IM, Larter SR (2003) The microbiology of hydrocarbon degradation in subsurface petroleum reservoirs: perspectives and prospects. *Research in Microbiology* **154**, 321–328.
Rosa C, Zeh J, George JC, Botta O, Zauscher M, Bada JL, O'Hara TM (2012) Age estimates based on aspartic acid racemization for bowhead whales (*Balaena mysticetus*) harvested in 1998–2000 and the relationship between racemization rate and body temperature. *Marine Mammal Science*, **29**, 424–445.
Schippers A, Neretin L, Kallmeyer J, Ferdelman T, Cragg B, Parkes R, Jørgensen B (2005) Prokaryotic cells of the deep sub-seafloor biosphere identified as living bacteria. *Nature* **433**, 861–864.
Schleifer KH, Kandler O (1972) Peptidoglycan types of bacterial cell walls and their taxonomic implications. *Bacteriological Reviews* **36**, 407–477.
Scholten JCM, Conrad R (2000) Energetics of syntrophic propionate oxidation in defined batch and chemostat cocultures. *Applied and Environmental Microbiology* **66**, 2934–2942.
Staudenbauer W (1968) D-aspartic acid incorporation into interpeptide bridges in bacterial cell wall. *Federation Proceedings* **27**, 294.
Stetter KO, Huber R, Blochl E, Kurr M, Eden RD, Fielder M, Cash H, Vance I (1993) Hyperthermophilic Archaea are thriving in deep North-Sea and Alaskan oil-reservoirs. *Nature* **365**, 743–745.
Stouthamer AH (1979) The search for correlation between theoretical and experimental growth yields. In *Microbial Biochemistry* (ed Quayle JR). University Park Press, Baltimore, MD, pp. 1–47.
Takahata Y, Hoaki T, Maruyama T (2001) Starvation survivability of *Thermococcus* strains isolated from Japanese oil reservoirs. *Archives of Microbiology* **176**, 264–270.
Takai K, Moser DP, DeFlaun MF, Onstott TC, Fredrickson JK (2001) Archaeal diversity in waters from deep South African Gold mines. *Applied and Environmental Microbiology* **67**, 5750–5760.
Takai K, Nakamura K, Toki T, Tsunogai U, Miyazaki M, Miyazaki J, Hirayama H, Nakagawa S, Nunoura T, Horikoshi K (2008) Cell proliferation at 122°C and isotopically heavy CH_4 production by a hyperthermophilic methanogen under high-pressure cultivation. *Proceedings of the National Academy of Sciences of the USA* **105**, 10949–10954.
Takano Y, Sato R, Kaneko T, Kobayashi K, Marumo K (2003) Biological origin for amino acids in a deep subterranean hydrothermal vent, Toyoha mine, Hokkaido, Japan. *Organic Geochemistry* **34**, 1491–1496.
Tijhuis L, vanLoosdrecht MCM, Heijnen JJ (1993) A thermodynamically based correlation for maintenance Gibbs energy requirements in aerobic and anaerobic chemotrophic growth. *Biotechnology and Bioengineering* **42**, 509–519.
Tomizawa H, Yamada H, Wada K, Imoto T (1995) Stabilization of lysozyme against irreversible inactivation by suppression of chemical reactions. *Journal of Biochemistry* **117**, 635–640.
VerEecke HC, Butterfield DA, Huber JA, Lilley MD, Olsond EJ, Roe KK, Evans LJ, Merkel AY, Cantin HV, Holden JF (2012) Hydrogen-limited growth of hyperthermophilic methanogens at deep-sea hydrothermal vents. *Proceedings of the National Academy of Sciences of the USA* **109**, 13674–13679.
Vieille C, Zeikus GJ (2001) Hyperthermophilic enzymes: sources, uses, and molecular mechanisms for thermostability. *Microbiology and Molecular Biology Reviews* **65**, 1–43.
van de Vossenberg JLCM, Ubbink-Kok T, Elferink MGL, Driessen AJM, Konings WN (1995) Ion permeability of the cytoplasmic membrane limits the maximum growth temperature of bacteria and archaea. *Molecular Microbiology*, **18**, 925–932.
van derWal A, Norde W, Bendinger B, Zehnder AJB, Lyklema J (1997) Chemical analysis of isolated cell walls of Gram-positive

bacteria and determination of the cell wall to cell mass ratio. *Journal of Microbiological Methods* **28**, 147–157.
Ward JA, Slater GF, Moser DP, Lin L-H, Lacrampe-Couloume G, Bonin AP, Davidson M, Hall JA, Mislowack B, Bellamy RES, Onstott TC, Sherwood Lollar B (2004) Microbial hydrocarbon gases in the witwatersrand basin, south africa: implications for the deep biosphere. *Geochimica et Cosmochimica Acta* **68**, 3239–3250.
Whitman WB, Coleman DC, Wiebe WJ (1998) Prokaryotes: the unseen majority. *Proceedings of the National Academy of Sciences of the USA* **95**, 6578–6583.
Wilhelms A, Larter SR, Head I, Farrimond P, di-Primio R, Zwach C (2001) Biodegradation of oil in uplifted basins prevented by deep-burial sterilization. *Nature* **411**, 1034–1037.
Willey JM, Sherwood LM, Woolverton CJ (2011) *Prescott's Microbiology*. McGraw-Hill Education, New York, NY, 1012100101.
Yamauchi T, Choi S-Y, Oikada H, Yohda M, Kumagai H, Esaki N, Soda K (1992) Properties of aspartate racemase, a pyridoxal 5′-phosphate-independent amino acid racemase. *Journal of Biological Chemistry*, **267**, 18361–18364.
Zhao M, Bada JL (1995) Determination of α-dialkylamino acids and their enantiomers in geological samples by high-performance liquid chromatography after derivatization with a chiral adduct of o-phthaldialdehyde. *Journal of Chromatography A* **690**, 55–63.

SUPPORTING INFORMATION

Additional Supporting Information may be found in the online version of this article:

Appendix S1 Supplementary materials and methods.

Appendix: Supplementary Materials and Methods

Does Aspartic Acid Racemization Constrain the Depth Limit of the Subsurface Biosphere?

SI Figures

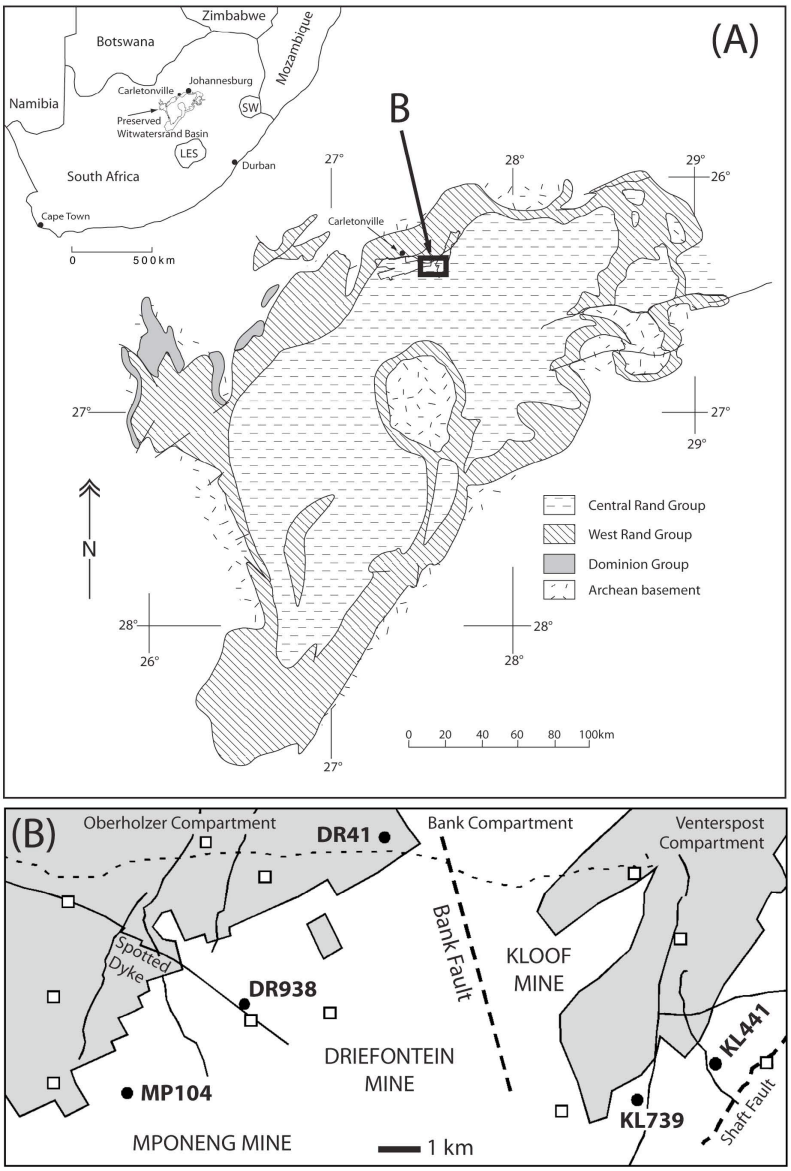

Fig. 1. Map of sampling locations. (A) Location of the Witwatersrand Basin in South Africa. (B) Location of South African sampling sites near Carletonville mining district.

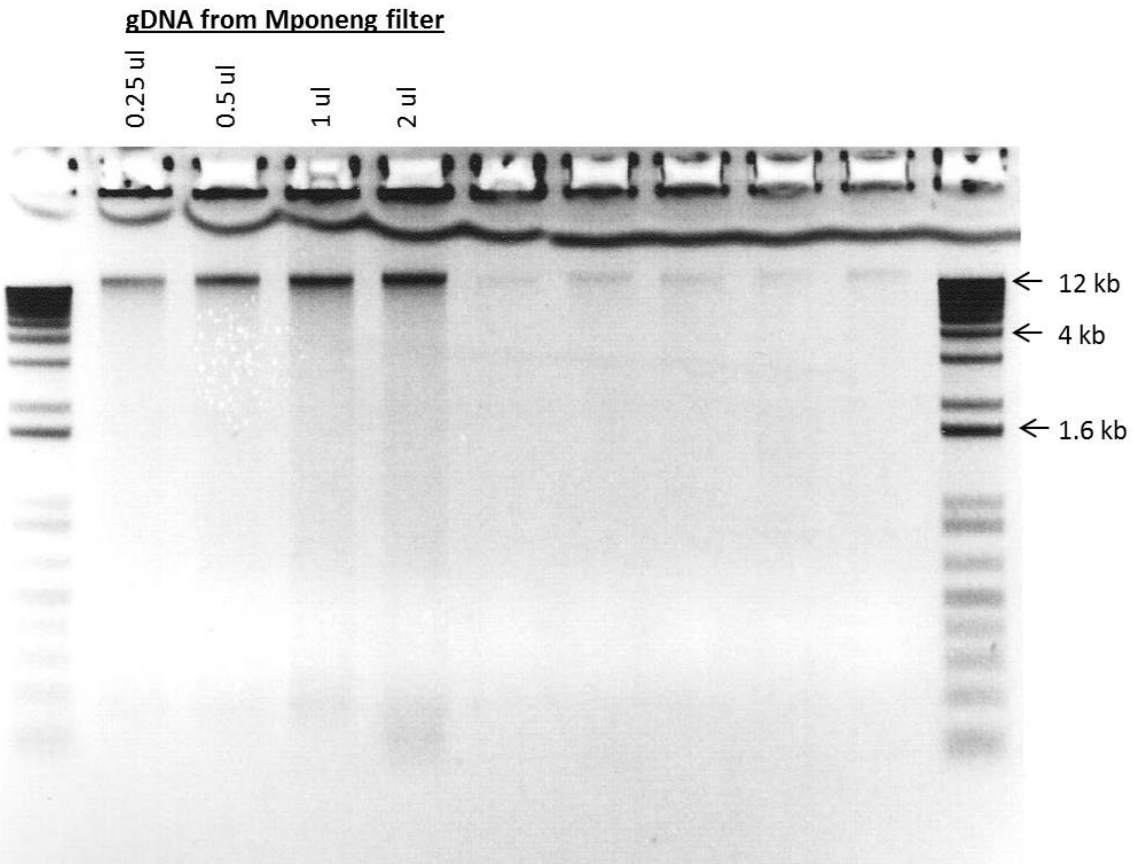

Fig. 2. Electrophoretic gel of genomic DNA extracted from the same filter used for amino acid analyses of sample MP104. Lanes on far left and far right indicate size of DNA. Four different volumes of DNA extract were analyzed, 0.25 mL to 2 mL. Most of the DNA was >10 kb with some smearing to shorter fragments.

SI Text

Model Parameters and Calculations. The rates for *in vivo* aspartic acid racemization must be adjusted to the water temperature for each filter sample (Table 1). The *in vivo* racemization rate constants were extrapolated to the borehole water temperatures using *in vivo* racemization data from Masters *et al.* (1977), which are similar those rates reported by Bada (1999) and Rosa *et al.* (2012). These extrapolations used an Arrhenius function for *in vivo* aspartic acid using the following equation,

$$k_{\mathrm{Asp}} = k_{\mathrm{T1}}\, e^{\frac{E_{\mathrm{A}}(T2-T1)}{RT1T2}} \qquad \text{(S1)}$$

where k_{T1} = 1.3±0.3x10^{-3} yr^{-1}, T1 = 37°C, E_{A} = 35±2 kcal mole^{-1}, R = 0.001986 kcal mole^{-1} K^{-1} and $T2$ is the *in situ* temperature in K. The standard deviation in k_{Asp} as a function of temperature was calculated using the following expression,

$$\sigma^2(k_{\mathrm{Asp}}) = \sigma^2(k_{\mathrm{T1}})\,[e^{\frac{E_{\mathrm{A}}(T2-T1)}{RT1T2}}]^2 + [\frac{E_A(T_2-T_1)}{RT_2T_1}]^2\,\sigma^2(E_{\mathrm{A}}) \quad \text{(S2)}$$

The error in the doubling time, t_{Asp}, and minimum metabolic rate, V, was then propagated from the error in the racemization rate of aspartic acid.

A steady-state between amino acid production and racemization is assumed to exist in these fracture water sites given that the estimated fracture water ages greatly exceed the half-life for aspartic acid racemization. In the case of the simple numerical model, the k_{TO} was manually adjusted until the D/L of aspartic acid stabilized and matched that of the measured D/L of aspartic acid. The steady-state assumption that the D/L is constant requires that the rate of newly produced L-aspartic acid matches the rate of D-aspartic acid production by racemization. This requirement can be expressed by combining equations (3) and (4) of the main text to yield the cellular protein turnover rate (k_{TO}) associated with the microbial community for a constant D/L for aspartic acid,

$$d\,(\mathrm{D/L})_{\mathrm{Asp}}/dt = 0 \quad \text{(S3)}$$

or,

$$\frac{d}{dt}\left[\frac{[(D_{\mathrm{Asp}})_{\mathrm{t}} + k_{\mathrm{Asp}}\,(L_{\mathrm{Asp}} - D_{\mathrm{Asp}})_{\mathrm{t}}\;t]}{[\,(L_{\mathrm{Asp}})_{\mathrm{t}} + [k_{\mathrm{TO}}\,(L_{\mathrm{Asp}})_{\mathrm{t}} + \;k_{\mathrm{Asp}}\;(D_{\mathrm{Asp}} - L_{\mathrm{Asp}})_{\mathrm{t}}]\;t]}\right] = 0 \quad \text{(S4)}$$

$$[k_{\mathrm{Asp}}\,(L_{\mathrm{Asp}} - D_{\mathrm{Asp}})_{\mathrm{t}}][\,(L_{\mathrm{Asp}})_{\mathrm{t}} + (k_{\mathrm{TO}}\,(L_{\mathrm{Asp}})_{\mathrm{t}} + \;k_{\mathrm{Asp}}\;(D_{\mathrm{Asp}} - L_{\mathrm{Asp}})_{\mathrm{t}}\,)t] - [(D_{\mathrm{Asp}})_{\mathrm{t}} + k_{\mathrm{Asp}}\,(L_{\mathrm{Asp}} - D_{\mathrm{Asp}})_{\mathrm{t}}\;t][k_{\mathrm{TO}}\,(L_{\mathrm{Asp}})_{\mathrm{t}} + \;k_{\mathrm{Asp}}\;(D_{\mathrm{Asp}} - L_{\mathrm{Asp}})_{\mathrm{t}}] = 0 \quad \text{(S5)}$$

$$[k_{\mathrm{Asp}}\,(L_{\mathrm{Asp}} - D_{\mathrm{Asp}})_{\mathrm{t}}][\,(1 + k_{\mathrm{TO}}\,t)(L_{\mathrm{Asp}})_{\mathrm{t}} - \;k_{\mathrm{Asp}}\;(L_{\mathrm{Asp}} - D_{\mathrm{Asp}})_{\mathrm{t}}\;t] - [(D_{\mathrm{Asp}})_{\mathrm{t}} + k_{\mathrm{Asp}}\,(L_{\mathrm{Asp}} - D_{\mathrm{Asp}})_{\mathrm{t}}\;t][k_{\mathrm{TO}}\,(L_{\mathrm{Asp}})_{\mathrm{t}} - \;k_{\mathrm{Asp}}\;(L_{\mathrm{Asp}} - D_{\mathrm{Asp}})_{\mathrm{t}}] = 0 \quad \text{(S6)}$$

$$k_{\mathrm{Asp}}\,(L_{\mathrm{Asp}} - D_{\mathrm{Asp}})_{\mathrm{t}}(1 + k_{\mathrm{TO}}\,t)(L_{\mathrm{Asp}})_{\mathrm{t}} - \;{k_{\mathrm{Asp}}}^2\;(L_{\mathrm{Asp}} - D_{\mathrm{Asp}})_{\mathrm{t}}{}^2\;t - (D_{\mathrm{Asp}})_{\mathrm{t}}k_{\mathrm{TO}}\,(L_{\mathrm{Asp}})_{\mathrm{t}} - \;k_{\mathrm{Asp}}\,k_{\mathrm{TO}}\,(L_{\mathrm{Asp}})_{\mathrm{t}}(L_{\mathrm{Asp}} - D_{\mathrm{Asp}})_{\mathrm{t}}\;t + (D_{\mathrm{Asp}})_{\mathrm{t}}k_{\mathrm{Asp}}\,(L_{\mathrm{Asp}} - D_{\mathrm{Asp}})_{\mathrm{t}} + {k_{\mathrm{Asp}}}^2\;(L_{\mathrm{Asp}} - D_{\mathrm{Asp}})_{\mathrm{t}}{}^2\;t = 0 \quad \text{(S7)}$$

$$k_{\mathrm{Asp}}\,(L_{\mathrm{Asp}} - D_{\mathrm{Asp}})_{\mathrm{t}}(L_{\mathrm{Asp}})_{\mathrm{t}} + k_{\mathrm{Asp}}k_{\mathrm{TO}}\,(L_{\mathrm{Asp}} - D_{\mathrm{Asp}})_{\mathrm{t}}(L_{\mathrm{Asp}})_{\mathrm{t}}\,t - (D_{\mathrm{Asp}})_{\mathrm{t}}k_{\mathrm{TO}}\,(L_{\mathrm{Asp}})_{\mathrm{t}} - \;k_{\mathrm{Asp}}\,k_{\mathrm{TO}}\,(L_{\mathrm{Asp}})_{\mathrm{t}}\,(L_{\mathrm{Asp}} - D_{\mathrm{Asp}})_{\mathrm{t}}\;t + (D_{\mathrm{Asp}})_{\mathrm{t}}\,k_{\mathrm{Asp}}(L_{\mathrm{Asp}} - D_{\mathrm{Asp}}) = 0 \quad \text{(S8)}$$

$$k_{\mathrm{Asp}}\,(L_{\mathrm{Asp}} - D_{\mathrm{Asp}})_{\mathrm{t}}(L_{\mathrm{Asp}})_{\mathrm{t}} - (D_{\mathrm{Asp}})_{\mathrm{t}}k_{\mathrm{TO}}\,(L_{\mathrm{Asp}})_{\mathrm{t}} + (D_{\mathrm{Asp}})_{\mathrm{t}}\,k_{\mathrm{Asp}}\,(L_{\mathrm{Asp}} - D_{\mathrm{Asp}})_{\mathrm{t}} = 0 \quad \text{(S9)}$$

$$k_{\mathrm{TO}}\,(D_{\mathrm{Asp}})_{\mathrm{t}}(L_{\mathrm{Asp}})_{\mathrm{t}} = k_{\mathrm{Asp}}\,(D_{\mathrm{Asp}})_{\mathrm{t}}(L_{\mathrm{Asp}} - D_{\mathrm{Asp}})_{\mathrm{t}} + \;k_{\mathrm{Asp}}\,(L_{\mathrm{Asp}} - D_{\mathrm{Asp}})_{\mathrm{t}}(L_{\mathrm{Asp}})_{\mathrm{t}} \quad \text{(S10)}$$

$$k_{\mathrm{TO}} = \frac{k_{\mathrm{Asp}}\;(D_{\mathrm{Asp}})_{\mathrm{t}}(L_{\mathrm{Asp}} - D_{\mathrm{Asp}})_{\mathrm{t}} + \;k_{\mathrm{Asp}}\,(L_{\mathrm{Asp}} - D_{\mathrm{Asp}})_{\mathrm{t}}(L_{\mathrm{Asp}})_{\mathrm{t}}}{(D_{\mathrm{Asp}})_{\mathrm{t}}(L_{\mathrm{Asp}})_{\mathrm{t}}} \quad \text{(S11)}$$

$$k_{\mathrm{TO}} = \frac{k_{\mathrm{Asp}}\,(L_{\mathrm{Asp}} + D_{\mathrm{Asp}}\,)_{\mathrm{t}}(L_{\mathrm{Asp}} - D_{\mathrm{Asp}})_{\mathrm{t}}}{(D_{\mathrm{Asp}})_{\mathrm{t}}(L_{\mathrm{Asp}})_{\mathrm{t}}} \quad \text{(S12)}$$

$$k_{\mathrm{TO}} = \frac{k_{\mathrm{Asp}}\;(1 + (D/L)_{\mathrm{Asp}})(L_{\mathrm{Asp}} - D_{\mathrm{Asp}})_{\mathrm{t}}}{(D_{\mathrm{Asp}})_{\mathrm{t}}}$$

$$k_{\mathrm{TO}} = k_{\mathrm{Asp}}\ (1 + (D/L)_{\mathrm{Asp}})((L/D)_{\mathrm{Asp}} - 1) \quad \text{(S13)}$$

(S14)

With this model the cellular protein grows exponentially at a rate k_{TO} for which the turnover time, $t_{\mathrm{Asp,}}$ is given by

$$t_{\mathrm{Asp}} = 1/k_{TO} \quad \text{(S15)}$$

The model is only dependent on the k_{Asp} and the D/L of aspartic acid in order to determine the turnover time of the cellular protein of the growing microbial community.

Alternatively, the protein generation rate could be a zero order constant and matched by a zero order protein decay associated with cell death and release of the protein into the extracellular pool. In this model the governing equation for the L-amino acids is as follows,

$$[\text{L-AA}]_{t+dt} = [\text{L-AA}]_t + [M_{\mathrm{TO}} + k_{RAC}\cdot[\text{D-AA}]_t - k_{RAC}\cdot[\text{L-AA}]_t - M_{\mathrm{TO}}\,[\text{L-AA}]_t/[\,[\text{L-AA}]_t+[\text{D-AA}]_t\,]\,]\,dt \quad \text{(S16)}$$

where M_{TO} is the L-amino acid generation rate (ng L^{-1} yr^{-1}) and $M_{TO}[\text{L-AA}]_t/[[\text{L-AA}]_t+[\text{D-AA}]_t]$ is the rate of old L-amino acid protein destruction (ng L^{-1} yr^{-1}). This simplifies to the following,

$$[\text{L-AA}]_{t+dt} = [\text{L-AA}]_t + [k_{RAC}\cdot[[\text{D-AA}]_t - [\text{L-AA}]_t] + M_{\mathrm{TO}}[\text{D-AA}]_t/[[\text{L-AA}]_t+[\text{D-AA}]_t]]\cdot dt \quad \text{(S17)}$$

The corresponding governing equation for the D-amino acids is,

$$[\text{D-AA}]_{t+dt} = [\text{D-AA}]_t + [k_{RAC}\cdot[[\text{L-AA}]_t - [\text{D-AA}]_t]] - M_{\mathrm{TO}}[\text{D-AA}]_t/[[\text{L-AA}]_t+[\text{D-AA}]_t]\cdot dt \quad \text{(S18)}$$

Restricting the model to aspartic acid equation S3 becomes the following,

$$\frac{d}{dt}\left[\frac{[(D_{\mathrm{Asp}})_{\mathrm{t}} + k_{\mathrm{Asp}}\,(L_{\mathrm{Asp}} - D_{\mathrm{Asp}})_{\mathrm{t}}\ t - M_{\mathrm{TO}}\,fD_{\mathrm{Asp}}\,t]}{[\,(L_{\mathrm{Asp}})_{\mathrm{t}} + k_{\mathrm{Asp}}\ (D_{\mathrm{Asp}} - L_{\mathrm{Asp}})_{\mathrm{t}}\,t + M_{\mathrm{TO}}\,fD_{\mathrm{Asp}}\,t\,]}\right] = 0 \quad \text{(S19)}$$

where $fD_{\mathrm{Asp}} = D_{\mathrm{Asp}}/[D_{\mathrm{Asp}}+L_{\mathrm{Asp}}]$, the fraction of D_{Asp} in the cellular aspartic acid pool. Differentiation yields the following,

$$[k_{\mathrm{Asp}}\,(L_{\mathrm{Asp}} - D_{\mathrm{Asp}})_{\mathrm{t}} - M_{\mathrm{TO}}\,fD_{\mathrm{Asp}}\,][\,(L_{\mathrm{Asp}})_{\mathrm{t}} + (k_{\mathrm{Asp}}\ (D_{\mathrm{Asp}} - L_{\mathrm{Asp}})_{\mathrm{t}}\,)t + M_{\mathrm{TO}}\,fD_{\mathrm{Asp}}\,t] - [k_{\mathrm{Asp}}\ (D_{\mathrm{Asp}} - L_{\mathrm{Asp}})_{\mathrm{t}} + M_{\mathrm{TO}}\,fD_{\mathrm{Asp}}\,][(D_{\mathrm{Asp}})_{\mathrm{t}} + k_{\mathrm{Asp}}(L_{\mathrm{Asp}} - D_{\mathrm{Asp}})_{\mathrm{t}}\ t - M_{\mathrm{TO}}\,fD_{\mathrm{Asp}}\,t] = 0 \quad \text{(S20)}$$

$$[k_{\mathrm{Asp}}\,(L_{\mathrm{Asp}} - D_{\mathrm{Asp}})_{\mathrm{t}} - M_{\mathrm{TO}}\,fD_{\mathrm{Asp}}\,][\,(L_{\mathrm{Asp}})_{\mathrm{t}} + (k_{\mathrm{Asp}}\,(D_{\mathrm{Asp}} - L_{\mathrm{Asp}})_{\mathrm{t}}\,)t + M_{\mathrm{TO}}\,fD_{\mathrm{Asp}}\,t] + [k_{\mathrm{Asp}}\,(L_{\mathrm{Asp}} - D_{\mathrm{Asp}})_{\mathrm{t}} - M_{\mathrm{TO}}\,fD_{\mathrm{Asp}}\,][(D_{\mathrm{Asp}})_{\mathrm{t}} + k_{\mathrm{Asp}}\,(L_{\mathrm{Asp}} - D_{\mathrm{Asp}})_{\mathrm{t}}t - M_{\mathrm{TO}}\,fD_{\mathrm{Asp}}\,t] = 0 \quad \text{(S21)}$$

$$[k_{\mathrm{Asp}}(L_{\mathrm{Asp}})_{\mathrm{t}}(L_{\mathrm{Asp}}-D_{\mathrm{Asp}})_{\mathrm{t}}-M_{\mathrm{TO}}\,(L_{\mathrm{Asp}})_{\mathrm{t}}fD_{\mathrm{Asp}}\,]$$
$$+\;[k_{\mathrm{Asp}}\,(D_{\mathrm{Asp}})_{\mathrm{t}}(L_{\mathrm{Asp}}-D_{\mathrm{Asp}})_{\mathrm{t}}-M_{\mathrm{TO}}\,(D_{\mathrm{Asp}})_{\mathrm{t}}fD_{\mathrm{Asp}}\,]=0 \tag{S22}$$

$$k_{\mathrm{Asp}}(L_{\mathrm{Asp}}+D_{\mathrm{Asp}})_{\mathrm{t}}(L_{\mathrm{Asp}}-D_{\mathrm{Asp}})_{\mathrm{t}}-M_{\mathrm{TO}}\,(L_{\mathrm{Asp}}+D_{\mathrm{Asp}})_{\mathrm{t}}fD_{\mathrm{Asp}}\;=0 \tag{S23}$$

$$M_{\mathrm{TO}}\;=\frac{k_{\mathrm{Asp}}\,(L_{\mathrm{Asp}}-D_{\mathrm{Asp}})_{\mathrm{t}}}{fD_{\mathrm{Asp}}} \tag{S24}$$

since $fD_{\mathrm{Asp}} = D_{\mathrm{Asp}}/[D_{\mathrm{Asp}}+L_{\mathrm{Asp}}]$, then

$$M_{\mathrm{TO}}\;=\frac{k_{\mathrm{Asp}}\,(L_{\mathrm{Asp}}-D_{\mathrm{Asp}})_{\mathrm{t}}(L_{\mathrm{Asp}}+D_{\mathrm{Asp}})_{\mathrm{t}}}{D_{\mathrm{Asp}}} \tag{S25}$$

$$\frac{M_{\mathrm{TO}}}{(L_{\mathrm{Asp}}+D_{\mathrm{Asp}})_{\mathrm{t}}}=\frac{k_{\mathrm{Asp}}(L_{\mathrm{Asp}}-D_{\mathrm{Asp}})_{\mathrm{t}}}{D_{\mathrm{Asp}}}=k_{\mathrm{Asp}}\,(L_{\mathrm{Asp}}/D_{\mathrm{Asp}}-1) \tag{S26}$$

since by definition $D_{\mathrm{Asp}}+L_{\mathrm{Asp}}$ is constant, then

$$k_{\mathrm{TO}}=\frac{M_{\mathrm{TO}}}{(L_{\mathrm{Asp}}+D_{\mathrm{Asp}})_{\mathrm{t}}}=k_{\mathrm{Asp}}\,(1/(D_{\mathrm{Asp}}/L_{\mathrm{Asp}})-1) \tag{S27}$$

For $D_{\mathrm{Asp}}/L_{\mathrm{Asp}} << 1$ this k_{TO} is virtually identical to the former k_{TO} as confirmed by numerical modeling.